Systems/Circuits

Role of Parafacial Nuclei in Control of Breathing in Adult Rats

Robert T.R. Huckstepp, Kathryn P. Cardoza, Lauren E. Henderson, and Jack L. Feldman
Department of Neurobiology, David Geffen School of Medicine, University of California, Los Angles, Los Angeles, California 90095-1763

Contiguous brain regions associated with a given behavior are increasingly being divided into subregions associated with distinct aspects of that behavior. Using recently developed neuronal hyperpolarizing technologies, we functionally dissect the parafacial region in the medulla, which contains key elements of the central pattern generator for breathing that are important in central CO_2-chemoreception and for gating active expiration. By transfecting different populations of neighboring neurons with allatostatin or HM_4D $G_{i/o}$-coupled receptors, we analyzed the effect of their hyperpolarization on respiration in spontaneously breathing vagotomized urethane-anesthetized rats. We identify two functionally separate parafacial nuclei: ventral (pF_V) and lateral (pF_L). Disinhibition of the pF_L with bicuculline and strychnine led to active expiration. Hyperpolarizing pF_L neurons had no effect on breathing at rest, or changes in inspiratory activity induced by hypoxia and hypercapnia; however, hyperpolarizing pF_L neurons attenuated active expiration when it was induced by hypercapnia, hypoxia, or disinhibition of the pF_L. In contrast, hyperpolarizing pF_V neurons affected breathing at rest by decreasing inspiratory-related activity, attenuating the hypoxia- and hypercapnia-induced increase in inspiratory activity, and when present, reducing expiratory-related abdominal activity. Together with previous observations, we conclude that the pF_V provides a generic excitatory drive to breathe, even at rest, whereas the pF_L is a conditional oscillator quiet at rest that, when activated, e.g., during exercise, drives active expiration.

Key words: **active expiration; control of breathing; expiratory oscillator; parafacial respiratory group; respiration; retrotrapezoid nucleus**

Introduction

Understanding how neurons are organized in microcircuits and networks is essential for comprehending behavior (Luo et al., 2008; Yuste, 2008). Here we exploit two related techniques for hyperpolarizing neurons to independently depress activity in neighboring populations of neurons and determined their role within the central pattern generator for breathing.

We hypothesize that breathing in mammals results from interactions between two oscillators (Mellen et al., 2003; Janczewski and Feldman, 2006; Feldman et al., 2013): the preBötzinger Complex (preBötC) is the kernel for inspiration (Smith et al., 1991; Tan et al., 2008), while the retrotrapezoid nucleus/parafacial respiratory group (RTN/pFRG), in whole or part, is vital for active expiration (Pagliardini et al., 2011) and CO_2-chemoreception (Smith et al., 1989; Li et al., 1999; Mulkey et al., 2004).

The RTN and pFRG are parafacial regions proximal to the ventral medullary surface that project to the ventral respiratory column (Smith et al., 1989; Ellenberger and Feldman, 1990; Pagliardini et al., 2011). One notable difference between them is that in newborn rodents pFRG but not RTN neurons are respiratory rhythmic (Onimaru and Homma, 2003); this activity begins to wane during the early neonatal period (Oku et al., 2007) and late expiratory activity is completely absent in both regions in adult rodents at rest (Pagliardini et al., 2011).

The discovery of a putative conditional RTN/pFRG oscillator driving active expiration (Mellen et al., 2003; Janczewski and Feldman, 2006) raised the question whether parafacial neurons responsible for chemoreception and active expiration are identical, overlap, or separate. That disinhibition or activation of mostly lateral parafacial neurons elicits active expiration (Pagliardini et al., 2011) led us to hypothesize that the pFRG and RTN are separable in adult rats.

Given that the respective anatomical parafacial boundaries and distinctive functional contributions of the RTN and pFRG are poorly defined, we use unbiased descriptors based on position relative to the facial motor nucleus. Thus we refer to lateral and ventral parafacial regions, i.e., pF_L and pF_V. We virally transfected pF_L and/or pF_V neurons to express distinctly different exogenous receptors, either the allatostatin receptor (AlstR; Birgül et al., 1999; Callaway, 2005) or the HM_4D receptor (HM_4DR; Nawaratne et al., 2008; Pei et al., 2008). Once these receptors are activated, transfected neurons are sufficiently hyperpolarized to become quiescent (Callaway, 2005; Tan et al., 2006, 2008; Nawaratne et al., 2008; Ray et al., 2011).

At rest when expiration is passive (Sherrey et al., 1988; Iizuka and Fregosi, 2007; Marina et al., 2010; Pagliardini et al., 2011), hyperpolarizing pF_L neurons had no effect on breathing patterns; during hypoxia or hypercapnia, which induce active expiration,

Received July 18, 2014; revised Nov. 6, 2014; accepted Nov. 8, 2014.
Author contributions: R.T.R.H. and J.L.F. designed research; R.T.R.H., K.P.C., and L.E.H. performed research; R.T.R.H. analyzed data; R.T.R.H. and J.L.F. wrote the paper.
This work was supported the National Institutes of Health.
The authors declare no competing financial interests.
Correspondence should be addressed to Jack L. Feldman, Box 951763, Department of Neurobiology, David Geffen School of Medicine, UCLA, Los Angeles, California 90095-1763. E-mail: feldman@ucla.edu.
DOI:10.1523/JNEUROSCI.2953-14.2015
 0270-6474/15/351052-16$15.00/0

Table 1. Table of abbreviations

Abbreviation	Definition
pF_V	Ventral parafacial region
pF_L	Lateral parafacial region
preBötC	PreBötzinger Complex
RTN	Retrotrapezoid nucleus
pFRG	Parafacial respiratory group
AlstR	Allatostatin receptor
Alst	Allatostatin
HM_4DR	HM_4D DREADD receptor
pF_L:HM_4DR	Lateral parafacial neurons transfected with HM_4D DREADD receptor
pF_V:AlstR	Ventral parafacial neurons transfected with allatostatin receptor
pF_V:HM_4DR	Ventral parafacial neurons transfected with HM_4D DREADD receptor
B + S	Bicuculline/strychnine
$B + S_{pF_L}$	Bicuculline/strychnine in the pF_L
CNO	Clozapine-*N*-oxide
T_I	Inspiratory duration
T_E	Expiratory duration
V_T	Tidal volume
Dia_{EMG}	Diaphragmatic electromyogram
GG_{EMG}	Genioglossal electromyogram
Abd_{EMG}	Abdominal electromyogram
f	Respiratory frequency

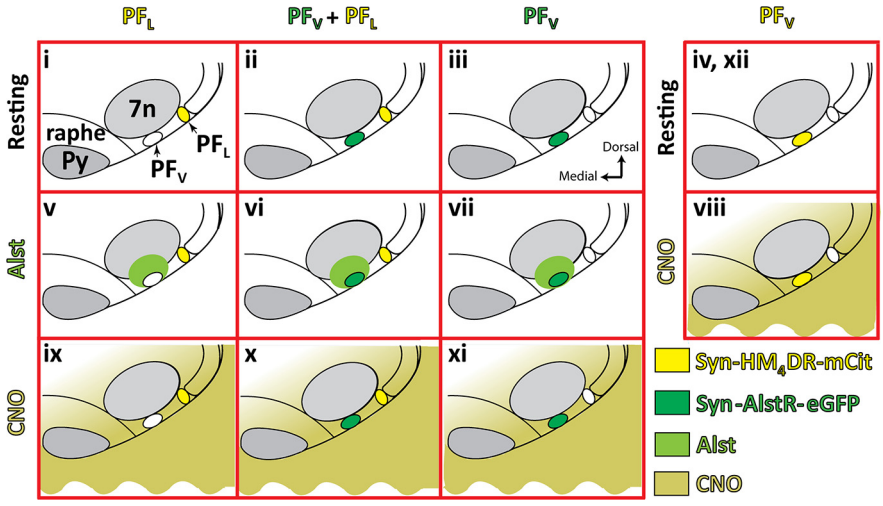

Figure 1. Overall experimental design. Rats were transfected with: syn-HM_4DR-mCit (light yellow) in ventral parafacial region (pF_V:HM_4DR) or into lateral parafacial region (pF_L:HM_4DR), or synapsin-AlstR-GFP (dark green) into pF_V (pF_V:AlstR), or both pF_L:HM_4DR and pF_V:AlstR. All rats were subject to the same triad of experimental challenges, i.e., hypoxia, hypercapnia, and disinhibition of pF_L. For rats transfected with pF_L:HM_4DR, pF_V:AlstR, or pF_L:HM_4DR and pF_V:AlstR, these challenges were performed under control conditions (***i–iii***), following injections of Alst (light green) into pF_V (***v–vii***), and following application of CNO (dark yellow) to medullary surface (***ix–xi***). Rats transfected with pF_V:HM_4DR underwent the same triad of experimental challenges, i.e., hypoxia, hypercapnia, and disinhibition of pF_L. These challenges were performed under control conditions (***iv***, before CNO; ***xii***, after CNO), and following application of CNO to medullary surface (***viii***). Data for different conditions were compared. Since Alst did not affect HM_4DR-transfected neurons and since CNO did not affect AlstR-transfected neurons, data for similar conditions were combined for analysis and comparisons. Thus we compared ***i*** + ***ii*** versus ***ix*** + ***x***, ***iii*** versus ***xi***, ***ii*** + ***iii*** versus ***vi*** + ***vii***, ***i*** versus ***v***, and ***iv*** + ***xii*** versus ***viii***.

hyperpolarizing pF_L neurons only attenuated expiratory activity; and disinhibition of the pF_L induced active expiration, and decreased frequency (*f*), which led to a concomitant increase in tidal volume (V_T), similar to photoactivation of pF_L neurons (Pagliardini et al., 2011). These effects are consistent with the pF_L acting as a conditional expiratory oscillator. Distinctly different responses were seen following hyperpolarizing pF_V neurons. At rest hyperpolarizing pF_V neurons decreased diaphragmatic EMG (Dia_{EMG}) amplitude, and reduced V_T with no change in *f*; during hypoxia or hypercapnia, hyperpolarizing pF_V neurons attenuated increases in inspiratory-related genioglossal and expiratory-related abdominal EMG amplitudes (GG_{EMG} and Abd_{EMG}, respectively), with no change in *f* or V_T; and following disinhibition of pF_L neurons, hyperpolarizing pF_V neurons reduced expiratory-related Abd_{EMG}, but did not affect the reduction in *f* or concomitant increase in V_T. Thus the pF_V appears to affect both inspiratory- and expiratory-related motor output, but does not appear to affect respiratory frequency. We conclude that the pF_L and pF_V are functionally distinct, with the pF_V providing an excitatory drive to breathe, even at rest, whereas the pF_L is a conditional oscillator, quiescent at rest, that when activated drives active expiration.

Materials and Methods

Viral design and handling. Two different viruses were used: AAV-2/5 hSyn-HA-hM_4D(Gi)-IRES-mCitrine (HM_4DR; University of North Carolina Gene Therapy Vector Core, Chapel Hill, NC) at a titer of 8×10^{12} vp/ml, and; AAV-DJ synapsin-allatostatin receptor-GFP (AlstR). We designed the latter virus using Nucleotide/Blast (NCBI, Bethesda, MD), University of Santa Cruz Genome Browser (UCSC, Santa Cruz, CA), Cister (Boston University, Boston, MA), and BioEdit (Ibis Biosciences). The insert (synapsin-SV40 SD/SA-AlstR) was synthesized (GenScript), and placed into the VPK 418 pAAV-IRES-GFP plasmid vector (Cell Biolabs), modified so that it lacked the CMV promoter and β-globin intron. The plasmid was then used to create a custom AAV-DJ virus (Salk Institute, GT[3] Core) at a titer of 5.8×10^{13} vp/ml. The viruses were aliquoted and stored at −80°C. On the day of injection, aliquots containing viruses were removed and held at 4°C, viruses were loaded by capillary action into glass pipettes, and pipettes containing viruses were placed into an electrode holder for pressure injection.

Viral transfection of pF_V and pF_L. All protocols were approved by the University of California Los Angeles Chancellor's Animal Research Committee. Male Sprague Dawley rats (350–450 g) were anesthetized by intraperitoneal injection of ketamine (100 mg/kg; Clipper Distribution), xylazine (10 mg/kg; Lloyd), and atropine (1 mg/kg; Westward Pharmaceutical); anesthesia was maintained with isoflurane (0.5–2%; Piramal Healthcare) throughout the procedure as required. Rats were placed in a prone position in a stereotaxic apparatus (Kopf Instruments) on a heating pad (TCAT 2-LV; Physitemp) and body temperature was maintained at a minimum of 36.5°C via a thermocouple. The head was leveled and glass pipettes were placed stereotaxically into the pF_V or pF_L (Figs. 1, 2). The pF_V was defined as the area ventral to the caudal half of the facial nucleus, between the pyramidal tract and the spinal trigeminal tract (coordinates: 1.8 mm lateral and 11.4 mm caudal from bregma, and 9.4 mm ventral from the surface of the cerebellum; Fig. 2*Ai*). The pF_L was defined as the area ventral to the lateral edge of the facial nucleus, juxtaposed to the spinal trigeminal tract (coordinates: 2.5 mm lateral and 11.1 mm caudal from bregma, and 9.2 mm ventral from the surface of the cerebellum; Fig. 2*Ai*). The virus solutions were pressure injected (100–150 nl) bilaterally using a Picospritzer II (General Valve) controlled by a Master 8 pulse generator (A.M.P.I.). Pipettes were left in place for 3–5 min to prevent back flow of the virus solution up the pipette track.

There were four virus injection protocols (Fig. 1): (1) HM_4DR in pF_L neurons (pF_L:HM_4DR), (2) AlstR in pF_V neurons (pF_V:AlstR), (3) Both

pF_L:HM_4DR and pF_V:AlstR (pF_L:HM_4DR + pF_V:AlstR), and (4) HM_4DR in pF_V neurons (pF_V:HM_4DR).

Postoperatively, rats received buprenorphine (0.1 mg/kg; Reckitt Benckiser) intraperitoneally and meloxicam (2 mg/kg; Norbrook) subcutaneously, followed by 10 d of oral antibiotics (TMS; Hi-Tech Pharmacal) and 4 d of oral meloxicam (0.05 mg/ml) in their drinking water. Rats were allowed 3–6 weeks for recovery and viral expression, with food and water *ad libitum*.

Ventral approach. Anesthesia was induced with isoflurane and maintained throughout surgery with urethane (Fig. 2*Aii*; 1.2–1.7 g/kg; Sigma) diluted in standard sterile saline (0.9% NaCl; Hospira) via a femoral catheter: urethane anesthesia was vital to seeing expiratory-related abdominal activity, as activity was not seen when isoflurane or ketamine were used (data not shown). Rats were placed supine onto a stereotaxic apparatus on a heating pad and core body temperature was maintained at a minimum of 36.5°C via a thermocouple. The trachea was cannulated. Respiratory flow was monitored via a flow head connected to a transducer (GM Instruments) and CO_2 via a capnograph (Type 340; Harvard Apparatus) connected to the tracheal tube. Paired EMG wire electrodes (Cooner Wire) were inserted into the genioglossus, diaphragm, and oblique abdominal muscles to record respiratory-related activity. After the anterior neck muscles were removed, a basio-occipital craniotomy exposed the ventral medullary surface, and the dura was resected. After bilateral vagotomy, the exposed tissue around the neck and the mylohyoid muscle was covered with dental putty (Reprosil; Dentsply Caulk) to prevent drying. The rat was left for 30 min to allow baseline recordings to stabilize.

At resting levels, ventilation was continuous, consisting of alternation of active contraction of inspiratory muscles, e.g., diaphragm, and passive expiration. Active expiration was initiated by substituting various gas mixtures for room air, i.e., hypoxia (8% O_2 and 92% N_2) or hypercapnia (9% CO_2, 21% O_2, and 70% N_2), or by disinhibition within the pF_L with the $GABA_A$ antagonist, bicuculline methobromide (250 μM; Tocris Bioscience) combined with the glycine antagonist strychnine hydrochloride (250 μM; Sigma-Aldrich) diluted in standard sterile saline.

All experiments began by testing responses to hypoxia, hypercapnia, and pF_L disinhibition [via injection of bicuculline/strychnine (B + S) in the pF_L (B + S_{pFL})] under resting conditions (Fig. 1*i–iv*). Rats were exposed to 1 min of hypoxia followed by a 15 min recovery period breathing room air, then changed to 2 min of hypercapnia after which rats were allowed 20 min breathing room air for baseline recordings to stabilize. Finally, rats received bilateral B + S_{pFL} followed by a 30 min recovery period while breathing room air. pF_L coordinates via a ventral approach were as follows: 2.5 mm lateral from the basilar artery, 0.9 mm rostral from the most rostral hypoglossal nerve rootlet, and 0.2 mm dorsal from the ventral surface. The B + S solution was pressure injected (50–100 nl) bilaterally using a Picospritzer II controlled by a Master 8 pulse generator. To avoid disruption of the tissue the B + S solution was injected at ~60 nl/min.

After experiments were performed under resting conditions, rats transfected with pF_V:AlstR or pF_L:HM_4DR + pF_V:AlstR were given a

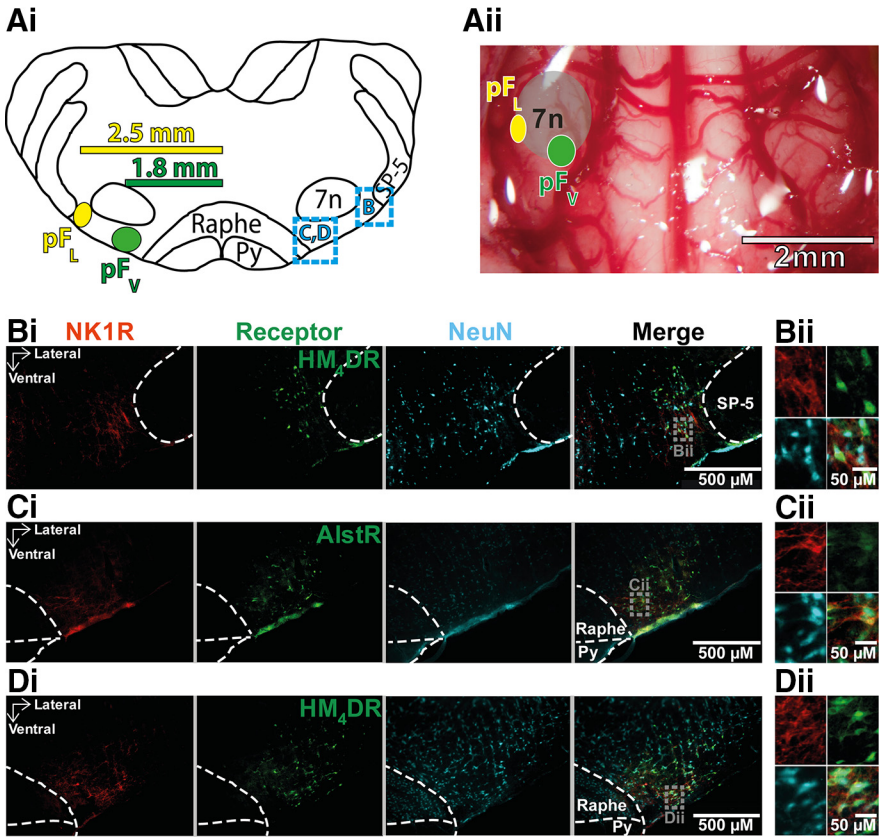

Figure 2. Neuronal transfection in parafacial regions. ***A***, Localization of injections into pF_V and pF_L. ***Ai***, Transverse view of medulla at bregma −11.25 mm. Dashed squared blue boxes identify location of sections illustrating immunocytochemistry shown in ***B–D***. ***Aii***, Ventral view of medullary surface. ***Ai***, ***Aii***, Green circle shows location of AlstR injection sites for pF_V (***Ci***),yellow circle shows location of HM_4DR injection sites for pF_L (***Bi***) and pF_V (***Di***). ***Bi–Di***, Micrographs of injection sites: neurons (blue) transfected with AlstR (in ***Ci***) expressing GFP, or HM_4DR (in ***Bi***, ***Di***) expressing mCitrine, colocalized with NK1R (red). ***Bii–Dii***, Expanded micrographs from merged figures in ***Bi–Di*** (dashed gray boxes): NeuN (blue), GFP, or mCitrine (green), and NK1R (red). Py, pyramidal tract; SP-5, spinal trigeminal tract; 7n, facial nucleus.

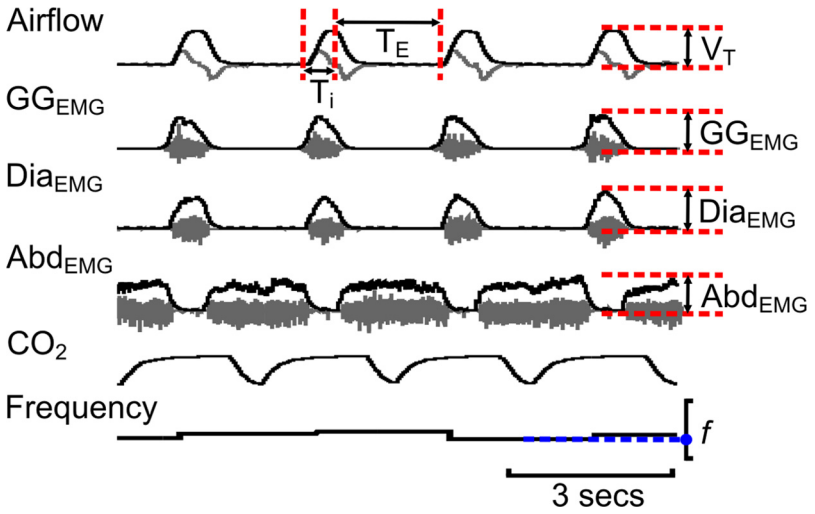

Figure 3. Measurement of respiratory variables. Gray traces are raw data (not shown in Figs. 4–13). Black traces are integrated data, end-tidal CO_2, and frequency (shown in Figs. 4–13). Maximum and minimum values for each variable were measured from integrated traces (red dashed lines) and the differences, along with frequency (blue line + dots), were used to calculate f, T_I, T_E, V_T, GG_{EMG}, Dia_{EMG}, and Abd_{EMG}.

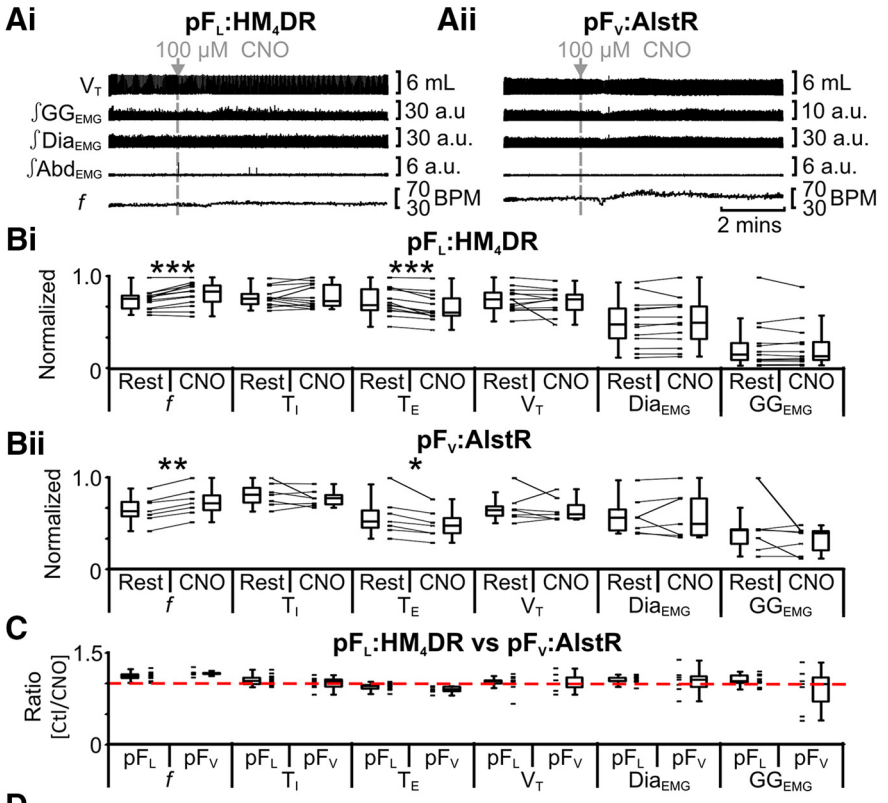

D

Values: median, IQR	*f* (breath/min)	T_I (secs)	T_E (secs)	V_T (mL)	Dia_{EMG}	GG_{EMG}
Rest (pF$_L$)	49.9, 9.2	0.3, 0.1	0.9, 0.3	3.9, 0.9	16.6, 11.3	6.9, 8.3
CNO (pF$_L$)	55.0, 11.7	0.3, 0.1	0.8, 0.2	3.8, 0.8	17.2, 12.2	6.1, 8.9
P=	0.0009	0.7	0.0002	0.9	0.1	0.8
Rest (pF$_V$)	48.5, 11.8	0.3, 0.1	0.9, 0.3	3.7, 0.6	20.0, 7.9	14.7, 5.3
CNO (pF$_V$)	55.1, 12.1	0.3, 0.0	0.8, 0.3	3.4, 0.8	17.6, 14.0	13.7, 7.0
P=	0.008	0.5	0.02	0.7	0.7	0.5
Ratio (pF$_L$)	1.1, 0.1	1.0, 0.1	0.9, 0.1	1.0, 0.1	1.0, 0.1	1.0, 0.1
Ratio (pF$_V$)	1.1, 0.0	1.0, 0.1	0.9, 0.1	1.0, 0.1	1.0, 0.2	0.9, 0.4
P=	0.06	0.5	0.06	0.8	0.8	0.5

Figure 4. Effect of CNO in rats with and without HM$_4$DRs. ***A***, Integrated traces: gray arrows and vertical dashed lines indicate application of CNO in pF$_L$:HM$_4$DR rats (***Ai***) or in rats lacking HM$_4$DRs, i.e., pF$_V$:AlstR rats (***Aii***). ***B***, Comparison of respiratory variables before and after CNO in pF$_L$:HM$_4$DR rats (***Bi***) and pF$_V$:AlstR rats (***Bii***). Lines connect data from individual experiments, and box-and-whisker plots show combined data. Data in ***Bi*** and ***Bii*** are normalized to highest value for that parameter, i.e., *f*, T_I, T_E, V_T, GG_{EMG}, Dia_{EMG}, or Abd_{EMG}, regardless of whether it belonged to control or CNO group. ***C***, Comparison of ratio changes between effects of CNO on pF$_L$:HM$_4$DR and pF$_V$:AlstR rats. Box-and-whisker plots show combined data, with data points from individual experiments. Data in ***C*** are expressed as ratios of resting values, and red horizontal dashed line represents a ratio of 1. ***D***, Table containing median, IQR, and *p* values, from data represented in ***A***. $*p < 0.05$, $**p < 0.01$, $***p < 0.005$.

bilateral injection of Alst (10 μM; Antagene) diluted in standard sterile saline into the pF$_V$ to test the effects of inactivation of the pF$_V$ (Fig. 1*vi*,*vii*), and rats transfected with pF$_L$:HM$_4$DR were given Alst to test for nonspecific effects of Alst in rats that lack the AlstR (Fig. 1*v*). pF$_V$ coordinates via a ventral approach were as follows: 1.8 mm lateral from the basilar artery, 0.6 mm rostral from the most rostral hypoglossal nerve rootlet, and 0.2 mm dorsal from the ventral surface. At 10 min post Alst, the response to hypoxia was re-examined. Additional Alst, with a 5 min stabilization period, preceded subsequent retesting of, first, the response to hypercapnia, and second, B + S_{pFL}. Then, after sufficient time for breathing to return to baseline levels (~30 min), clozapine-N-oxide (CNO; 100 μM; Santa Cruz Biotechnology) diluted in standard sterile saline was applied to the ventral medullary surface of rats transfected with pF$_L$:HM$_4$DR + pF$_V$:AlstR or pF$_L$:HM$_4$DR to test the effects of pF$_L$ inactivation (Fig. 1*ix*,*x*), and CNO was applied to the ventral medullary surface of rats transfected with pF$_V$:AlstR to test for nonspecific effects of CNO in rats that lack the HM$_4$DR (Fig. 1*xi*); to allow breathing to stabilize, measurements were taken after 10 min. Then, the rats were again tested for responses to hypoxia, hypercapnia, and B + S_{pFL}, with CNO reapplied 5 min before each test.

As there was no difference in the responses to pF$_L$ inactivation in rats transfected with pF$_L$:HM$_4$DR (Fig. 1*ix*) or pF$_L$:HM$_4$DR + pF$_V$:AlstR (Fig. 1*x*), the data from both groups were combined for analysis. As there was also no difference in the responses to Alst in rats transfected with pF$_V$:AlstR (Fig. 1*vii*) or pF$_L$:HM$_4$DR + pF$_V$:AlstR (Fig. 1*vi*), the data from both groups were combined for analysis. Thus experiments represented by Figure 1, *i* and *ii*, were compared with *ix* and *x*, *iii* were compared with *xi*, *ii* + *iii* were compared with *vi* + *vii*, and *i* were compared with *v*.

Rats transfected with HM$_4$DR in the pF$_V$, i.e., pF$_V$:HM$_4$DR rats, were only tested for their response to CNO. As for other experiments, we measured the responses under resting conditions to hypoxia and hypercapnia. Then, after sufficient time for breathing to return to baseline levels (~30 min), CNO was applied to the ventral medullary surface to test the effects of pF$_V$ inactivation (Fig. 1*viii*); to allow breathing to stabilize, measurements were taken after 10 min. Then, the rats were again tested for responses to hypoxia and hypercapnia, with CNO reapplied 5 min before each test. Finally, after washing off the CNO, the protocol was repeated a third time, again under resting conditions. The pre-experimental and post-experimental conditions were averaged for control data used for analysis (Fig. 1*iv*,*xii*).

Localization of transfected neurons. Rats were killed by an overdose of urethane and transcardially perfused using a peristaltic pump (Cole Palmer) with saline followed by cold (4°C) paraformaldehyde (PFA; 4%; Thermo Fischer Scientific). The medulla was harvested and postfixed in 4% PFA overnight at 4°C, then cryoprotected in sucrose (30%; Thermo Fischer Scientific) in standard PBS (1–3 d at 4°C). PBS contained the following (in mM): 137 NaCl, 2.7 KCl, 10 Na_2HPO_4, and 1.8 KH_2PO_4, adjusted to pH 7.4 with HCl (all reagents from Thermo Fischer Scientific).

Brainstems were transversely sectioned at 40 μm with a cryostat (Leica Biosystems). Free-floating sections were incubated overnight in PBS containing 0.1% Triton X-100 (PBT) and the following primary antibodies (1:500): mouse anti-NeuN (EMD Millipore), rabbit anti-neurokinin 1 receptor (NK1R; EMD Millipore), and chicken anti- GFP (Aves Labs). The tissue was washed in PBS six times for 5 min per wash and then incubated separately for 2–4 h in a solution of PBT containing the following secondary antibodies (1:250): donkey anti-mouse Alexa Fluor 647, donkey anti-rabbit rhodamine red, and donkey anti-chicken Alexa Fluor 488 (Jackson ImmunoResearch). The tissue was again washed in PBS six times for 5 min per wash. Slices were mounted onto polylysine-coated slides, dehydrated overnight at room temperature, and coverslipped using Cytoseal 60 (Electron Microscopy Sciences) mounting medium. Slides were observed under an AxioCam 2 Zeiss fluorescent microscope with AxioVision acquisition software (Zeiss). Images were acquired and exported as TIFF files.

To calculate the transfection efficiencies of the two viruses, we counted transfected neurons from a single representative 40 μm section at the core of the pF$_L$:HM$_4$DR ($n = 3$) and pF$_V$:AlstR ($n = 3$) injection sites from different rats. Images of these sections were opened in CorelDRAW

(Corel), and an ROI was drawn around the injection site. Then NeuN expression within the ROI was marked, using different colors, as being colocalized with a virally driven fluorophore (i.e., mCitrine or GFP) or not. The ROI containing the different colored marks was then exported as a TIFF file and cell counts were performed in ImageJ (NIH). Data were exported to Excel (Microsoft) for further analysis, and statistical analysis was performed in Igor Pro (WaveMetrics). Cell counts are expressed as mean and SD.

Data analysis and statistics. EMG signals and airflow measurements were collected using preamplifiers (P5; Grass) connected to a PowerLab AD board (ADInstruments) in a laboratory computer running LabChart software (ADInstruments), and were sampled at 400 Hz per channel. High-pass filtered (>0.1 Hz) flow head measurements were used to calculate: inspiratory duration (T_I), expiratory duration (T_E), and tidal volume (V_T). V_T was calculated as the change in amplitude of the integrated airflow signal during inspiration, converted to milliliters by comparison to calibration with a 3 ml syringe (Fig. 3). From the integrated airflow signal, T_I was measured from the beginning of inspiration until peak V_T, and T_E was measured from peak V_T to the beginning of the next inspiration (Fig. 3). Frequency (f) was ($1/(T_I+T_E)$; Fig. 3). EMG data were integrated ($\tau = 0.05$ s), and respiratory muscle activity was calculated as the peak amplitude of the integrated Dia_{EMG}, GG_{EMG}, and Abd_{EMG}, respectively (Fig. 3). There were two forms of activity seen on the GG_{EMG} trace: one phase locked with inspiration and the other phase locked with expiration. Inspiratory GG_{EMG} activity was present under all conditions tested, and as such GG_{EMG} measurements during the inspiratory phase of respiration are analyzed throughout this manuscript. Expiratory GG_{EMG} activity is not present at rest, but could be initiated during active expiration. As expiratory GG_{EMG} activity was not consistently induced by any of the above manipulations, either in the same preparation or between different preparations, these data were not included for further analysis. To obtain control values, the 20 cycles preceding each experimental manipulation for all parameters were averaged. Under hypoxic or hypercapnic conditions, measurements from the 20 cycles preceding stimulus cessation were averaged. As the time of the peak response to B + S_{pF_L} was different on each channel (airflow, Dia_{EMG}, GG_{EMG}, and Abd_{EMG}), for values for the effect of B + S_{pFL}, 20 cycles were averaged at the peak of change on each channel separately; all measurements from the integrated airflow channel (f, V_T, T_I, and T_E) were made from the same 20 cycles. Data were analyzed off-line, and then exported to Excel for further analysis. All statistical tests were performed using Igor Pro. In one pF_V:HM_4DR experiment, data were excluded from analysis from the GG_{EMG} channel, as the baseline was unstable in the period preceding the hypercapnic challenge.

For each variable, we calculated the ratio change induced by each stimulus under each condition. We divided the average of 20 cycles at the peak of the stimulus by the average of 20 cycles preceding the stimulus. These ratios were then used for statistical comparison. For example, to compute the ratio change for the effects of hyperpolarizing pF_L:HM_4DR neurons with CNO on respiratory changes induced by B + S_{pF_L} (1) we computed the ratio of the change of each variable induced by B + S_{pFL} compared with its control, which we designate as [B + S_{pF_L}/Ctl]; (2) we computed the ratio of the change of each variable induced by B + S_{pF_L} in the presence of CNO compared with its control in the presence of CNO, which we designate as [(B + S_{pF_L} + CNO)/(Ctl + CNO)]; and (3) we compared the ratio changes of both groups, i.e., [B + S_{pF_L}/Ctl] vs [(B + S_{pF_L} + CNO)/(Ctl + CNO)]. If the ratio change in the presence of CNO was significantly closer to 1, then we conclude hyperpolarizing pF_L:HM_4DR neurons reduced the effect of changes induced by B + S_{pF_L}. If the ratio change in the presence of CNO was significantly further away from 1, then we conclude hyperpolarizing pF_L:HM_4DR neurons potentiated the effect of changes induced by B + S_{pF_L}. If the ratio changes were not significantly different, then we conclude that hyperpolarizing pF_L:HM_4DR neurons did not modulate changes induced by B + S_{pF_L}. Ratios normalized datasets, which removed large differences in absolute values between datasets and led to fewer statistical outliers.

As described above, for each rat we calculated the average of 20 cycles preceding the stimulus ($\bar{X}_{control}$), and the average of 20 cycles during the stimulus ($\bar{X}_{stimulus}$). Both groups, the $\bar{X}_{control}$ values and their associated

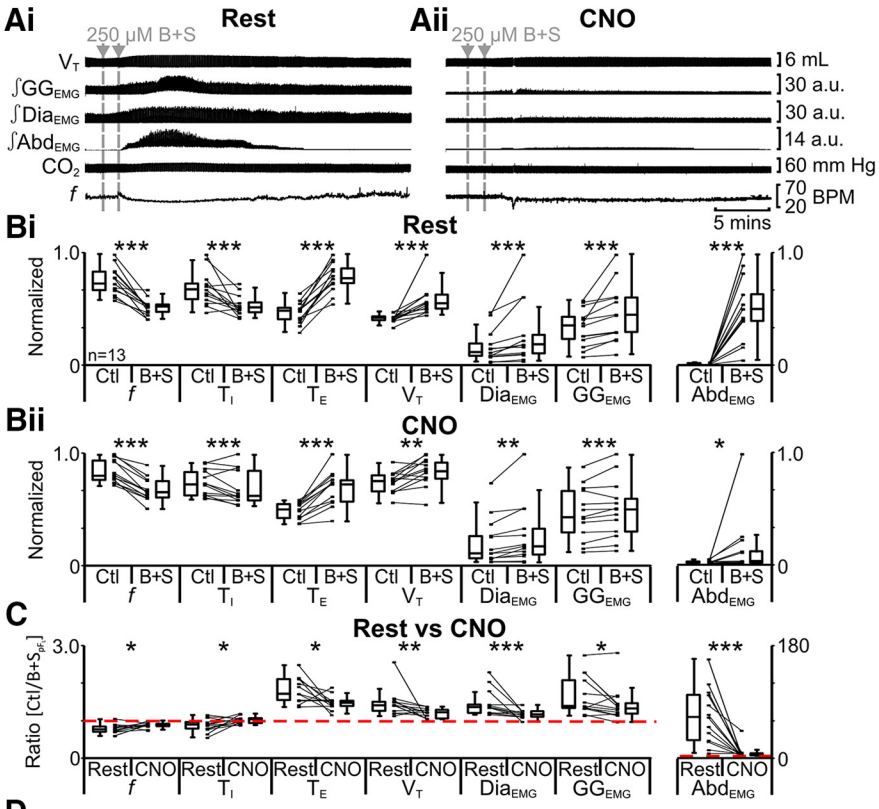

D

Values: median, IQR	*f* (breath/min)	T_I (secs)	T_E (secs)	V_T (mL)	Dia_{EMG}	GG_{EMG}	Abd_{EMG}
Rest	44.2, 9.6	0.4, 0.1	1.0, 0.2	4.1, 0.3	18.6, 10.6	8.4, 8.6	0.2, 0.1
B+S_{pF_L}	31.5, 3.7	0.3, 0.1	1.6, 0.3	5.4, 1.3	23.6, 16.5	13.6, 12.7	12.7, 6.1
P=	0.0002	0.003	0.0001	0.0002	0.0001	0.0001	0.0001
CNO	51.9, 11.2	0.4, 0.1	0.8, 0.2	3.7, 0.7	16.1, 13.9	5.7, 10.7	0.2, 0.1
CNO B+S_{pF_L}	43.7, 7.3	0.3, 0.1	1.1, 0.3	4.3, 0.8	18.6, 11.1	8.9, 12.2	0.3, 0.8
P=	0.0001	0.005	0.0001	0.003	0.007	0.0006	0.02
Ratio (B+S_{pF_L})	0.7, 0.1	0.8, 0.2	1.6, 0.6	1.3, 0.2	1.3, 0.2	1.3, 0.8	63.0, 73.5
Ratio (CNO B+S_{pF_L})	0.8, 0.1	1.0, 0.1	1.4, 0.1	1.1, 1.1	1.1, 0.2	1.3, 0.3	1.1, 3.6
P=	0.02	0.02	0.04	0.01	0.002	0.02	0.0002

Figure 5. Hyperpolarizing pF_L neurons significantly reduced effects of disinhibition of pF_L (B + S_{pF_L}). ***A***, Integrated traces from a single experiment: gray arrows and vertical dashed lines represent pipette placement for unilateral and bilateral B + S_{pF_L}. ***Ai***, Rest. ***Aii***, During application of CNO to medullary surface (present for entire trace). ***B***, Comparison of respiratory variables before and after B + S_{pF_L} in pF_L:HM_4DR rats at rest (***Bi***) and in the presence of CNO (***Bii***). Lines connect data from individual experiments, and box-and-whisker plots show combined data. Data in ***Bi*** and ***Bii*** are normalized to highest value for that parameter, i.e., *f*, T_I, T_E, V_T, GG_{EMG}, Dia_{EMG}, or Abd_{EMG}, regardless of whether it belonged to control or B + S_{pF_L} group. ***C***, Comparison between ratio changes induced by B + S_{pF_L} in pF_L:HM_4DR rats at rest and in the presence of CNO. Data in ***C*** are expressed as ratios of resting values, and red horizontal dashed line represents ratio of 1. ***D***, Table containing median, IQR, and *p* values, from data represented in ***B***. $*p < 0.05$, $**p < 0.01$, $***p < 0.005$.

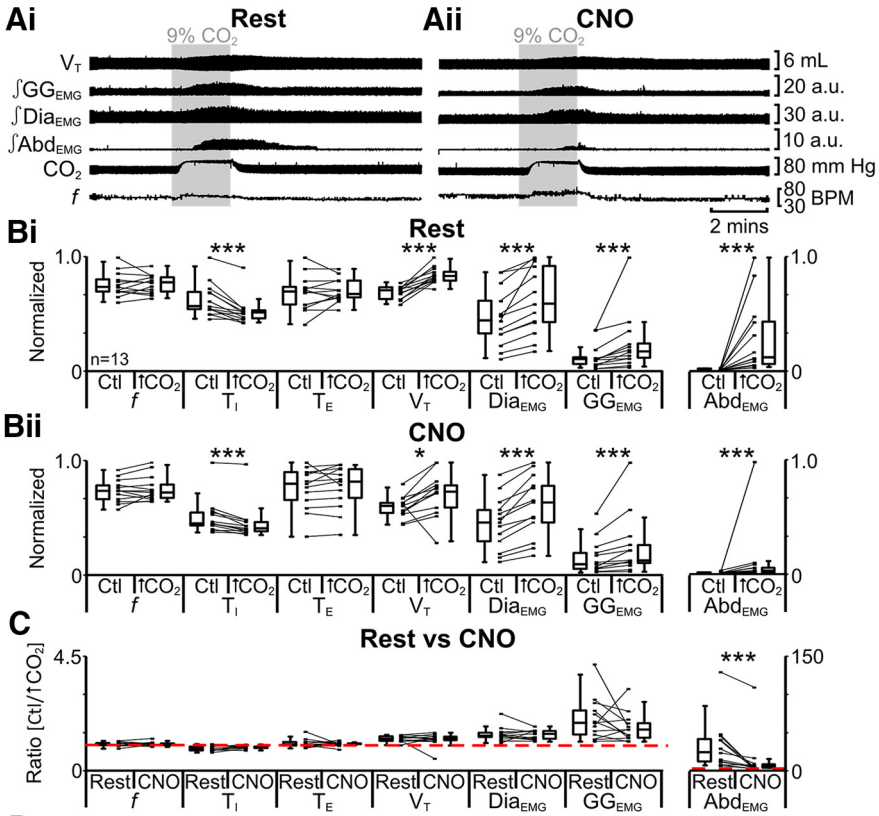

D

Values: median, IQR	*f* (breath/min)	T_I (secs)	T_E (secs)	V_T (mL)	Dia_{EMG}	GG_{EMG}	Abd_{EMG}
Rest	45.0, 6.4	0.34, 0.09	1.0, 0.2	4.4, 0.6	17.2, 11.5	9.6, 6.0	0.2, 0.1
9% CO_2	47.4, 7.9	0.30, 0.04	1.0, 0.2	5.1, 0.5	23.1, 19.5	16.5, 12.8	3.2, 10.8
P=	0.8	0.0008	0.4	0.0005	0.0001	0.0001	0.0001
CNO	53.3, 8.8	0.35, 0.09	0.8, 0.3	3.6, 0.6	17.1, 10.3	6.1, 9.6	0.2, 0.1
CNO 9% CO_2	52.4, 8.4	0.32, 0.06	0.8, 0.2	4.4, 1.2	23.7, 12.2	8.4, 11.0	0.7, 1.1
P=	0.3	0.0006	0.2	0.02	0.0002	0.0002	0.0002
Ratio (9% O_2)	1.0, 0.1	0.9, 0.2	1.0, 0.1	1.2, 0.2	1.2, 0.1	1.9, 1.0	21.7, 29.1
Ratio (CNO 9% CO_2)	1.0, 0.1	0.9, 0.1	1.0, 0.0	1.2, 0.1	1.3, 0.2	1.6, 0.6	3.0, 4.8
P=	0.5	0.2	0.6	1.0	0.7	0.3	0.0002

Figure 6. Hyperpolarizing pF_L neurons reduced effects of hypercapnia (9% CO_2) on Abd_{EMG} only. ***A***, Integrated traces from a single experiment: shaded area shows period of hypercapnia. ***Ai***, Rest. ***Aii***, During application of CNO to medullary surface (present for entire trace). ***B***, Comparison of respiratory variables before and after hypercapnia in pF_L:HM_4DR rats at rest (***Bi***) and in the presence of CNO (***Bii***). Lines connect data from individual experiments, and box-and-whisker plots show combined data. Data in ***Bi*** and ***Bii*** are normalized to highest value for that parameter, i.e., *f*, T_I, T_E, V_T, GG_{EMG}, Dia_{EMG}, or Abd_{EMG}, regardless of whether it belonged to control or 9% CO_2 group. ***C***, Comparison between ratio changes induced by hypercapnia in pF_L:HM_4DR rats at rest and in the presence of CNO. Data in ***C*** are expressed as ratios of resting values, and red horizontal dashed line represents a ratio of 1. ***D***, Table containing median, IQR, and *p* values, from data represented in ***B***. $*p < 0.05$, $**p < 0.01$, $***p < 0.005$.

$\bar{X}_{stimulus}$ value for every rat, were combined into a single dataset. To facilitate graphical comparisons, excluding ratio changes (see above), data were normalized to the highest value in the dataset regardless of whether it belonged to $\bar{X}_{control}$ or $\bar{X}_{stimulus}$ group. Therefore the highest value in the dataset, whether it be $\bar{X}_{control}$ or $\bar{X}_{stimulus}$, was 1.0.

For the purpose of analysis, active expiration was defined by the presence of bursts of Abd_{EMG} activity above tonic levels between inspiratory bursts, similar to previous studies (Pagliardini et al., 2011).

As usually seen in smaller sample sizes ($n < 30$), recorded data were often skewed, and thus were treated as nonparametric, for which the median and interquartile range (IQR) better represent the data than mean, and SD or SE. We used nonparametric tests for our statistical analysis, as these tests make fewer assumptions about the data and would not require us to exclude statistical outliers. Statistical tests are Wilcoxon signed-rank tests unless otherwise stated, with a significance level of $p \leq 0.05$. In Results, we have displayed the data as box-and-whisker plots for comparison of group data and as line graphs for individual experiments.

Results

Targeting of specific parafacial regions

By carefully choosing stereotaxic coordinates we were able to target viral injections into two anatomically separate regions that we designate as the parafacial ventral (pF_V) and parafacial lateral (pF_L; Fig. 2). Using anatomical markers we confirmed the location of our injections and that they were restricted to defined areas with no overlapping transfection of neurons (Fig. 2*B*,*C*). The pF_L was defined as the area ventral to the lateral edge of the facial nucleus, juxtaposed to the spinal trigeminal tract (Fig. 2*Ai*,*B*). The pF_V was defined as the area ventral to the caudal half of the facial nucleus, between the pyramidal tract and the spinal trigeminal tract (Fig. 2*Ai*,*C*,*D*). In representative individual 40 μm sections from the core of the synapsin-HM_4DR injection site in the pF_L of different rats, 135 ± 20 neurons expressed mCitrine representing 78 ± 9% of neurons ($n = 3$). Similarly, in representative individual 40 μm sections from the core of the synapsin-AlstR injection site in the pF_V of different rats, 129 ± 21 neurons expressed GFP, representing 76 ± 6% of neurons ($n = 3$). Therefore, the transfection efficiencies of the two viruses in each area were similar for both the number of transfected neurons ($p = 0.5$), and the percentage of neurons transfected ($p = 0.3$).

Hyperpolarizing pF_L neurons at rest had no effect on breathing

Based on our hypothesis that in adult rat the pF_L is a conditional expiratory oscillator that is inactive at rest (Janczewski and Feldman, 2006; Pagliardini et al., 2011), we predicted little or no effect of hyperpolarizing pF_L neurons on resting ventilation. In anesthetized rats at rest transfected with HM_4DR in the lateral parafacial, i.e., pF_L:HM_4DR rats (Fig. 1*ix*,*x*), CNO increased frequency (*f*) and decreased expiratory period (T_E), with no significant effect on inspiratory period (T_I), tidal volume (V_T), Dia_{EMG}, or GG_{EMG}; Abd_{EMG}, silent at rest, remained so after CNO ($n = 13$; Fig. 4*Ai*,*Bi*,*D*).

We assessed whether the effects of CNO on resting ventilation were due exclusively to actions via pF_L:HM_4DR-transfected neurons or confounded by nonspecific effects. In anesthetized rats at rest with no HM_4DRs (i.e., pF_V:AlstR rats; Fig. 1*xi*), CNO increased *f* and decreased T_E with no significant effect on T_I, V_T, Dia_{EMG}, and GG_{EMG}; Abd_{EMG}, silent at rest, remained so after CNO ($n = 7$; Fig. 4*Aii*,*Bii*,*D*). To determine whether hyperpolarizing pF_L:HM_4DR neurons had additional effects on *f* and T_E beyond the nonspecific effects seen in pF_V:AlstR rats, we computed for each measured variable, i.e., *f*, T_I, T_E, V_T, Dia_{EMG}, GG_{EMG}, and Abd_{EMG}, the ratio of its value after CNO divided by

its value before CNO, i.e., "ratio change" (see Materials and Methods, Data analysis and statistics), in rats with versus without HM_4DRs, i.e., pF_L:HM_4DR [(rest + CNO)/rest] vs pF_V:AlstR [(rest + CNO)/rest]. The ratio changes between the pF_L:HM_4DR and pF_V:AlstR rat groups were not significantly different for any variable ($n = 20$; Kruskal–Wallis; Fig. 4*C*,*D*). As the effects of CNO on resting ventilation were similar whether HM_4DRs were present or not, the CNO-induced changes at rest were not due to activation of HM_4DRs, but instead to some nonspecific effect of CNO or its vehicle. In subsequent experiments, to control for nonspecific effects of CNO, we compared the effects of CNO on the responses to different stimuli in rats without HM_4DRs to rats with HM_4DRs.

Disinhibition of pF_L has profound effects on respiration

pF_L neurons can be disinhibited by injection of a mixture of the $GABA_A$ and glycine antagonists bicuculline and strychnine (B + S_{pFL}), which results in a transformation in breathing from passive to active expiration (Pagliardini et al., 2011). Hyperpolarization of pF_L:HM_4DR neurons should reduce the depolarizing effects of B + S_{pFL}. In anesthetized rats at rest transfected with HM_4DR in the lateral parafacial, i.e., pF_L:HM_4DR rats (Fig. 1*i*,*ii*), B + S_{pFL} decreased f and T_I; increased T_E, V_T, Dia_{EMG}, and GG_{EMG}; and induced expiratory-related Abd_{EMG} ($n = 13$; Fig. 5*Ai*,*Bi*,*D*), the latter a signature of active expiration, q.v. (Pagliardini et al., 2011). The same trends ($n = 13$; Fig. 5*Aii*-,*Bii*,*D*) were seen in the presence of CNO (Fig. 1*ix*,*x*). However, in the presence of CNO following B + S_{pFL}, the ratio changes [(B + S_{pFL} + CNO)/(Ctl + CNO)] for all measured variables were significantly closer to 1 than those in the absence of CNO [B + S_{pFL}/Ctl] ($n = 13$; Fig. 5*C*,*D*). As CNO in the absence of HM_4DRs did not affect the response to B + S_{pFL} (see next paragraph), these results indicate that hyperpolarizing pF_L:HM_4DR neurons with CNO attenuated the effects of B + S_{pFL} on all variables.

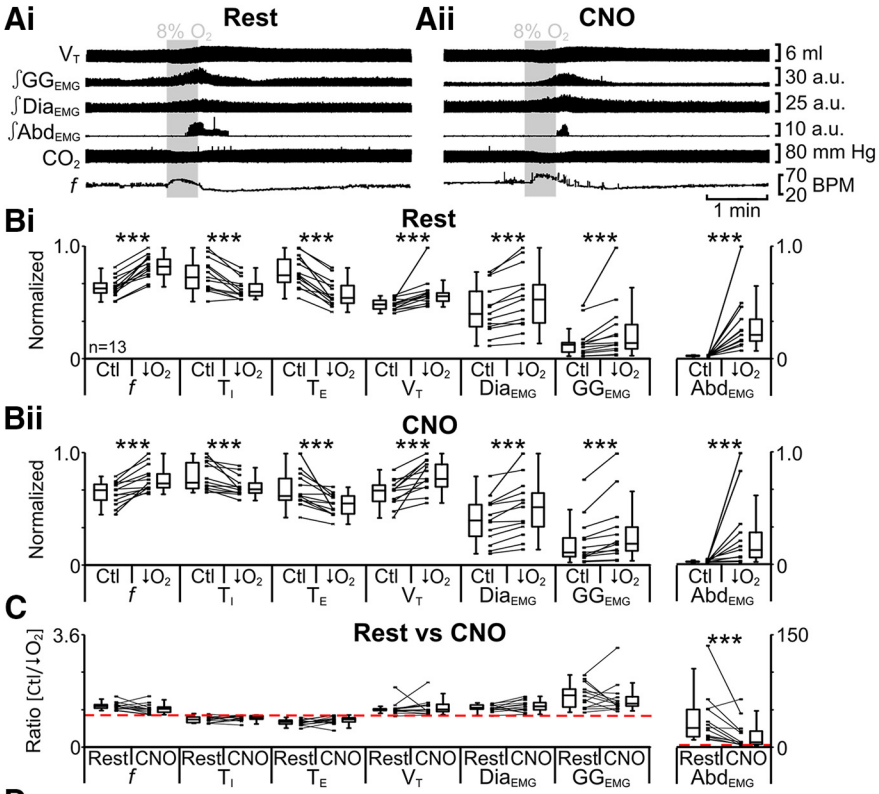

D

Values: median, IQR	*f* (breath/min)	T_I (secs)	T_E (secs)	V_T (mL)	Dia_{EMG}	GG_{EMG}	Abd_{EMG}
Rest	43.7, 6.2	0.35, 0.10	1.0, 0.3	4.2, 0.7	15.8, 12.5	10.8, 7.5	0.2, 0.1
8% O_2	57.5, 9.6	0.29, 0.05	0.7, 0.2	4.8, 0.5	20.8, 13.6	12.1, 19.4	4.7, 4.7
P=	0.0002	0.0005	0.0002	0.0005	0.0005	0.0002	0.0002
CNO	55.0, 11.7	0.32, 0.10	0.8, 0.2	3.8, 0.8	17.2, 12.2	6.1, 8.9	0.2, 0.1
CNO 8% O_2	60.0, 10.3	0.30, 0.04	0.7, 0.2	4.4 1.2	22.4, 13.0	10.2, 11.3	1.7, 3.2
P=	0.0002	0.0002	0.0002	0.0002	0.0002	0.0002	0.0002
Ratio (8% O_2)	1.3, 0.1	0.9, 0.2	0.8, 0.1	1.2, 0.1	1.2, 0.1	1.6, 0.6	24.0, 36.5
Ratio (CNO 8% O_2)	1.2, 0.2	0.9, 0.1	0.8, 0.1	1.2, 0.2	1.3, 0.2	1.4, 0.3	5.1, 18.0
P=	0.1	0.1	0.2	0.3	0.2	0.6	0.005

Figure 7. Hyperpolarizing pF_L neurons reduced effects of hypoxia (8% O_2) on Abd_{EMG} only. ***A***, Integrated traces from a single experiment: shaded area shows period of hypoxia. ***Ai***, Rest. ***Aii***, During application of CNO to medullary surface (present for entire trace). ***B***, Comparison of respiratory variables before and after hypoxia in pF_L:HM_4DR rats at rest (***Bi***) and in the presence of CNO (***Bii***). Lines connect data from individual experiments, and box-and-whisker plots show combined data. Data in ***Bi*** and ***Bii*** are normalized to highest value for that parameter, i.e., *f*, T_I, T_E, V_T, GG_{EMG}, Dia_{EMG}, or Abd_{EMG}, regardless of whether it belonged to control or 8% O_2 group. ***C***, Comparison between ratio changes induced by hypoxia in pF_L:HM_4DR rats at rest and in the presence of CNO. Data in ***C*** are expressed as ratios of resting values, and red horizontal dashed line represents a ratio of 1. ***D***, Table containing median, IQR, and *p* values, from data represented in ***B***. $*p < 0.05$, $**p < 0.01$, $***p < 0.005$.

CNO does not affect the response to B + S_{pFL} in the absence of CNO-sensitive HM_4DRs

In anesthetized rats at rest with no HM_4DRs, i.e., pF_V:AlstR rats (Fig. 1*iii*), B + S_{pFL} decreased f ($p = 0.02$) and T_I ($p = 0.02$), increased T_E ($p = 0.008$), V_T ($p = 0.02$), Dia_{EMG} ($p = 0.008$), and GG_{EMG} ($p = 0.008$), and induced expiratory-related Abd_{EMG} ($p = 0.02$; $n = 7$; data not shown). The same trends ($n = 7$; *f*: $p = 0.02$; T_I: $p = 0.02$; T_E: $p = 0.008$; V_T: $p = 0.02$; Dia_{EMG}: $p = 0.008$; GG_{EMG}: $p = 0.008$; Abd_{EMG}: $p = 0.02$; data not shown) were seen in the presence of CNO (Fig. 1*xi*). Importantly, in the presence of CNO following B + S_{pFL}, the ratio changes [(B + S_{pFL} + CNO)/(Ctl + CNO)] for all measured variables were not significantly different to those in the absence of CNO [B + S_{pFL}/Ctl] ($n = 7$; *f*: $p = 0.8$; T_I: $p = 0.2$; T_E: $p = 0.7$; V_T: $p = 1.0$; Dia_{EMG}: $p = 1.0$; GG_{EMG}: $p = 0.7$; Abd_{EMG}: $p = 0.6$; data not shown). Thus any nonspecific effects of CNO on *f* did not affect the response to B + S_{pFL}.

Hyperpolarizing pF_L neurons during hypercapnia only affect Abd_{EMG}

Hypercapnia increases ventilation by increasing V_T without a concurrent change in *f* (Stunden et al., 2001; Putnam et al., 2005), and elicits robust expiratory-related abdominal activity (Iizuka and Fregosi, 2007; Marina et al., 2010), i.e., active expiration. These effects were reduced by hyperpolarizing parafacial neurons (Marina et al., 2010). In anesthetized rats at rest transfected with

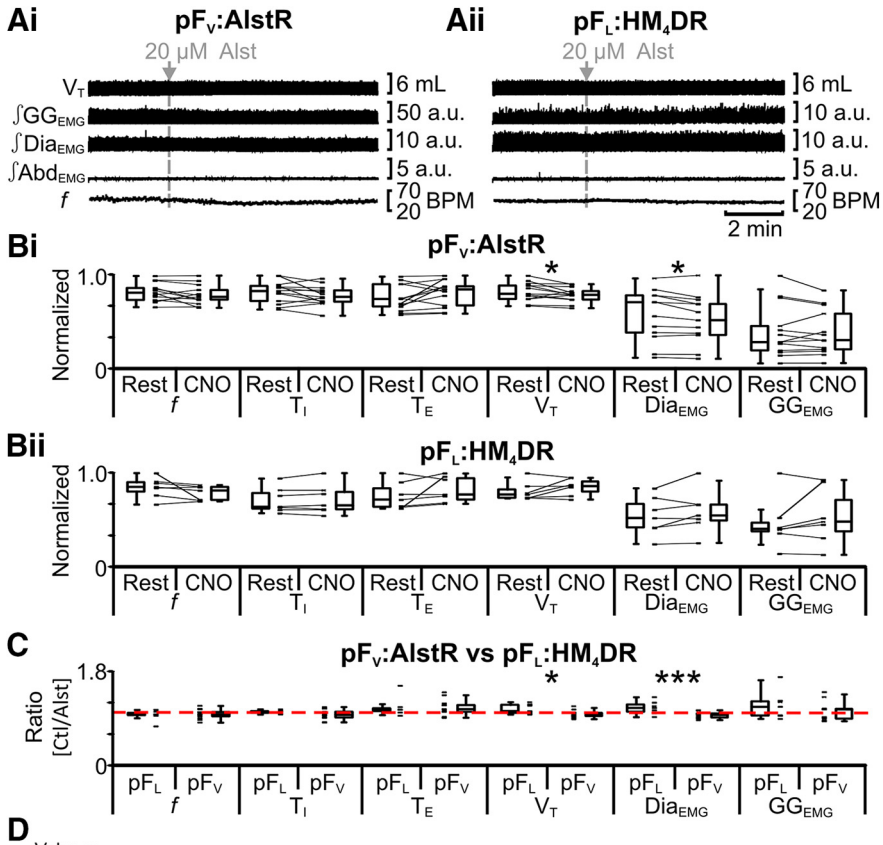

D

Values: median, IQR	*f* (breath/min)	T_I (secs)	T_E (secs)	V_T (mL)	Dia$_{EMG}$	GG$_{EMG}$
Rest (pF$_L$)	48.0, 5.4	0.3, 0.1	0.9, 0.2	4.2, 0.5	15.9, 7.2	5.5, 1.2
Alst (pF$_L$)	45.8, 7.5	0.3, 0.1	1.0, 0.3	4.7, 0.6	16.7, 4.9	6.5, 4.2
P=	0.1	0.7	0.2	0.4	0.2	0.4
Rest (pF$_V$)	46.7, 7.5	0.3, 0.1	1.0, 0.3	3.6, 0.7	24.0, 15.8	11.6, 11.0
Alst (pF$_V$)	44.1, 6.1	0.3, 0.1	1.1, 0.3	3.5, 0.4	21.6, 12.8	12.4, 16.0
P=	0.2	0.2	0.09	0.04	0.03	0.7
Ratio (pF$_L$)	1.0, 0.0	1.0, 0.0	1.1, 0.1	1.02, 0.12	1.1, 0.1	1.0, 0.2
Ratio (pF$_V$)	1.0, 0.1	1.0, 0.1	1.1, 0.1	0.96, 0.07	0.90, 0.1	1.1, 0.2
P=	0.8	0.2	1.0	0.02	0.005	0.2

Figure 8. pF$_V$ provides facilitative drive to respiration at rest. ***A***, Integrated traces from a single experiment: gray arrows and vertical dashed lines show the beginning of Alst injection in pF$_V$:AlstR rats (***Ai***), or in rats lacking AlstRs, i.e., pF$_L$:HM$_4$DR rats (***Aii***). ***B***, Comparison of respiratory variables before and after Alst in pF$_V$:AlstR rats (***Bi***) and pF$_L$:HM$_4$DR rats (***Bii***). Lines connect data from individual experiments, and box-and-whisker plots show combined data. Data in ***Bi*** and ***Bii*** are normalized to highest value for that parameter, i.e., *f*, T_I, T_E, V_T, GG$_{EMG}$, Dia$_{EMG}$, or Abd$_{EMG}$, regardless of whether it belonged to control or Alst group. ***C***, Comparison of ratio changes between effects of Alst on pF$_L$:HM$_4$DR and pF$_V$:AlstR rats. Box-and-whisker plots show combined data, with data points from individual experiments. Data in ***C*** are expressed as ratios of resting values, and red horizontal dashed line represents a ratio of 1. ***D***, Table containing median, IQR, and *p* values, from data represented in ***A***. $*p < 0.05$, $**p < 0.01$, $***p < 0.005$.

HM$_4$DR in the lateral parafacial, i.e., pF$_L$:HM$_4$DR rats (Fig. 1*i*,*ii*), hypercapnia did not affect *f*; decreased T_I; did not affect T_E; increased V_T, Dia$_{EMG}$, and GG$_{EMG}$; and induced expiratory-related Abd$_{EMG}$ ($n = 13$; Fig. 6*Ai*,*Bi*,*D*). The same trends ($n = 13$; Fig. 6*Aii*,*Bii*,*D*) were seen in the presence of CNO (Fig. 1*ix*,*x*). However, in the presence of CNO during hypercapnia only the ratio change [(hypercapnia + CNO)/(Ctl + CNO)] for expiratory-related Abd$_{EMG}$ was significantly closer to 1 than the ratio change in the absence of CNO [hypercapnia/Ctl] ($n = 13$; Fig. 6*C*,*D*). CNO in the absence of HM$_4$DRs did not affect the response to hypercapnia (see next paragraph). Thus hyperpolarizing pF$_L$:HM$_4$DR neurons with CNO attenuated the effects of hypercapnia only on expiratory-related Abd$_{EMG}$.

CNO does not affect the response to hypercapnia in the absence of CNO-sensitive HM$_4$DRs

In anesthetized rats at rest with no HM$_4$DRs, i.e., pF$_V$:AlstR rats (Fig. 1*iii*), hypercapnia did not affect *f* ($p = 1.0$); decreased T_I ($p = 0.04$); did not affect T_E ($p = 0.6$); increased V_T ($p = 0.02$), Dia$_{EMG}$ ($p = 0.008$), and GG$_{EMG}$ ($p = 0.008$); and induced expiratory-related Abd$_{EMG}$ ($p = 0.008$; $n = 7$; data not shown). The same trends ($n = 7$; *f*: $p = 0.6$; T_I: $p = 0.02$; T_E: $p = 0.3$; V_T: $p = 0.02$; Dia$_{EMG}$: $p = 0.008$; GG$_{EMG}$: $p = 0.008$; Abd$_{EMG}$: $p = 0.008$; data not shown) were seen in the presence of CNO (Fig. 1*xi*). Importantly, during hypercapnia in the presence of CNO, the ratio changes [(hypercapnia + CNO)/(Ctl in CNO)] for all measured variables were not significantly different to those in the absence of CNO [hypercapnia/Ctl] ($n = 7$; *f*: $p = 1.0$; T_I: $p = 0.3$; T_E: $p = 0.7$; V_T: $p = 0.9$; Dia$_{EMG}$: $p = 0.4$; GG$_{EMG}$: $p = 0.1$; Abd$_{EMG}$: $p = 0.8$; data not shown). Thus any nonspecific effects of CNO on *f* did not affect the response to hypercapnia.

Hyperpolarizing pF$_L$ neurons during hypoxia only affect Abd$_{EMG}$

Hypoxia increases ventilation by increasing V_T with a concurrent change in *f*, and elicits robust expiratory-related abdominal activity (Sherrey et al., 1988; Iizuka and Fregosi, 2007). In anesthetized rats at rest transfected with HM$_4$DR in the lateral parafacial, i.e., pF$_L$:HM$_4$DR rats (Fig. 1*i*,*ii*), hypoxia increased *f*; decreased T_I and T_E; increased V_T, Dia$_{EMG}$, and GG$_{EMG}$; and induced expiratory-related Abd$_{EMG}$ ($n = 13$; Fig. 7*Ai*,*Bi*,*D*). The same trends ($n = 13$; Fig. 7*Aii*,*Bi*,*D*) were seen in the presence of CNO (Fig. 1*ix*;*x*). However, in the presence of CNO during hypoxia only the ratio change [(hypoxia + CNO)/(Ctl + CNO)] for expiratory-related Abd$_{EMG}$ was significantly closer to 1 than the ratio change in the absence of CNO [hypoxia/Ctl] ($n = 13$; Fig. 7*C*,*D*). CNO in the absence of HM$_4$DRs did not affect the response to hypoxia (see next paragraph). Thus hyperpolarizing pF$_L$:HM$_4$DR neurons with CNO only attenuated the effects of hypoxia on expiratory-related Abd$_{EMG}$.

CNO does not affect response to hypoxia in absence of CNO-sensitive HM$_4$DRs

In anesthetized rats at rest with no HM$_4$DRs, i.e., pF$_V$:AlstR rats (Fig. 1*iii*), hypoxia increased *f* ($p = 0.02$); decreased T_I ($p = 0.04$) and T_E ($p = 0.04$); increased V_T ($p = 0.02$), Dia$_{EMG}$ ($p = 0.008$), and GG$_{EMG}$ ($p = 0.008$); and induced expiratory-related Abd$_{EMG}$ ($p = 0.008$; $n = 7$; data not shown). The same trends ($n = 7$; *f*: $p =$

0.02; T_I: $p = 0.04$; T_E: $p = 0.04$; V_T: $p = 0.02$; Dia_{EMG}: $p = 0.008$; GG_{EMG}: $p = 0.008$; Abd_{EMG}: $p = 0.008$; data not shown) were seen in the presence of CNO (Fig. 1*xi*). Importantly, in the presence of CNO, during hypoxia, the ratio changes [(hypoxia + CNO)/(Ctl + CNO)] for all measured variables were not significantly different to the ratio changes in the absence of CNO [hypoxia/Ctl] ($n = 7$; *f*: $p = 0.5$; T_I: $p = 0.1$; T_E: $p = 0.9$; V_T: $p = 0.3$; Dia_{EMG}: $p = 0.9$; GG_{EMG}: $p = 0.2$; Abd_{EMG}: $p = 0.7$; data not shown). Thus any nonspecific effect of CNO on *f* did not affect the response to hypoxia.

Hyperpolarizing pF_V neurons at rest decrease V_T and Dia_{EMG}

Neurons ventral to the facial nucleus are hypothesized to provide significant ventilatory drive at rest (Smith et al., 1989; Ellenberger and Feldman, 1990; Nattie, 2000; Guyenet et al., 2005), and hyperpolarizing neurons ventral to the facial nucleus decrease resting ventilation (Nattie and Li, 2002; Li et al., 2006) and reduce phrenic nerve activity (Marina et al., 2010). Thus we predicted that hyperpolarizing pF_V neurons would reduce Dia_{EMG} and consequently V_T. In anesthetized rats at rest transfected with AlstR in the ventral parafacial, i.e., pF_V:AlstR rats (Fig. 1*vi*,*vii*), allatostatin bilaterally injected into the pF_V (Alst) decreased V_T and Dia_{EMG}, with no significant effect on *f*, T_I, T_E, and GG_{EMG}; Abd_{EMG}, silent at rest, remained so after Alst ($n = 13$; Fig. 8*Ai*,*Bi*,*D*).

We assessed whether the effects of injecting Alst into the pF_V on resting ventilation were due exclusively to actions via pF_V:AlstR neurons or confounded by nonspecific effects of Alst or vehicle. In anesthetized rats at rest with no AlstRs, i.e., pF_L:HM_4DR rats (Fig. 1*v*), Alst did not affect *f*, T_I, T_E, V_T, Dia_{EMG}, and GG_{EMG}; Abd_{EMG}, silent at rest, remained so after Alst ($n = 7$; Fig. 8*Aii*,*Bii*,*D*). Therefore, following Alst under resting conditions only the ratio changes, i.e., pF_V:AlstR [(rest + Alst)/rest] vs pF_L:HM_4DR [(rest + Alst)/rest], for V_T and Dia_{EMG} in pF_V:AlstR rats were significantly different to those in pF_L:HM_4DR rats ($n = 20$; Kruskal–Wallis; Fig. 8*C*,*D*). Thus hyperpolarizing pF_V:AlstR neurons reduced V_T and Dia_{EMG}, consistent with the hypothesis that the pF_V contributes to respiratory drive at rest (Smith et al., 1989; Ellenberger and Feldman, 1990).

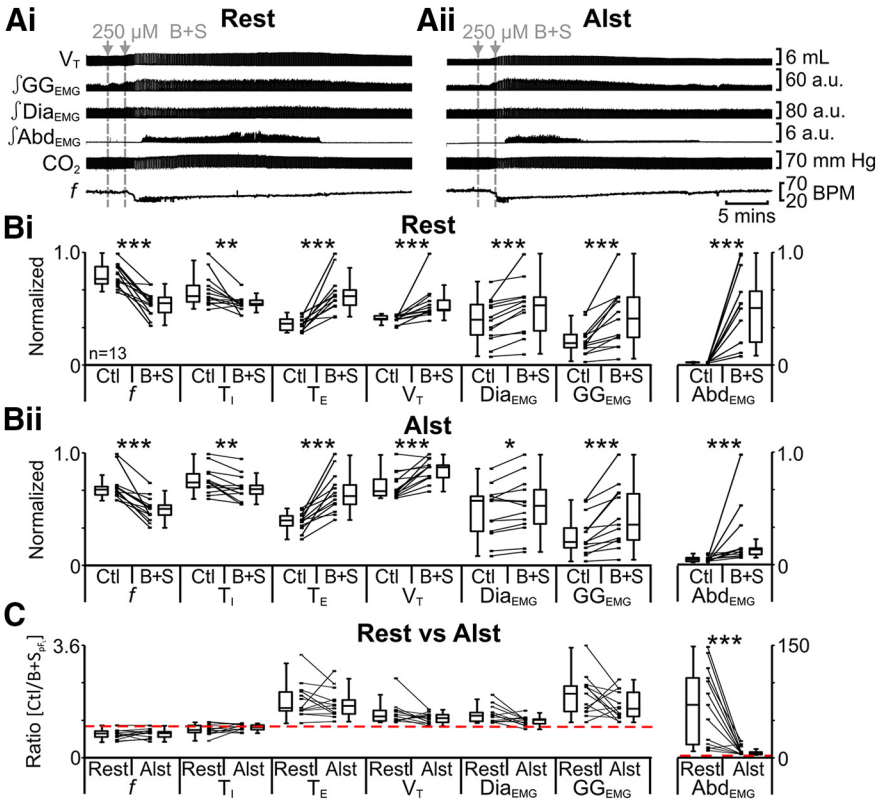

D

Values: median, IQR	*f* (breath/min)	T_I (secs)	T_E (secs)	V_T (mL)	Dia_{EMG}	GG_{EMG}	Abd_{EMG}
Rest	41.6, 8.4	0.32, 0.08	1.1, 0.3	3.9, 0.3	21.1, 14.3	14.3, 8.8	0.2, 0.1
B+S_{pF_L}	29.7, 7.4	0.28, 0.02	1.8, 0.4	4.7, 0.7	27.8, 16.2	30.9, 27.2	12.7, 11.7
P=	0.0002	0.009	0.0001	0.0002	0.0001	0.0001	0.0001
Alst	51.3, 5.4	0.31, 0.05	0.9, 0.2	3.1, 0.7	23.5, 12.8	9.6, 8.2	0.2, 0.1
Alst B+S_{pF_L}	38.3, 6.6	0.28, 0.02	1.3, 0.4	4.1, 0.5	21.8, 12.5	16.8, 19.1	0.6, 0.2
P=	0.0002	0.009	0.0001	0.001	0.02	0.0001	0.0002
Ratio (B+S_{pF_L})	0.7, 0.2	0.8, 0.2	1.5, 0.6	1.3, 0.3	1.3, 0.3	2.0, 0.8	67.3, 88.8
Ratio (Alst B+S_{pF_L})	0.7, 0.2	0.9, 0.1	1.6, 0.5	1.2, 0.3	1.2, 0.1	1.5, 0.8	2.2, 3.1
P=	0.4	0.3	0.5	0.2	0.07	0.1	0.001

Figure 9. Hyperpolarizing pF_V neurons reduced effects of disinhibition of pF_L (B + S_{pF_L}) on Abd_{EMG} only. ***A***, Integrated traces from a single experiment: gray arrows and vertical dashed lines represent pipette placement for unilateral and bilateral B + S_{pF_L}. ***Ai***, Rest. ***Aii***, After Alst in pF_V (present for entire trace). ***B***, Comparison of respiratory variables before and after B + S_{pF_L} in pF_V:AlstR rats at rest (***Bi***) and in the presence of Alst (***Bii***). Lines connect data from individual experiments, and box-and-whisker plots show combined data. Data in ***Bi*** and ***Bii*** are normalized to highest value for that parameter, i.e., *f*, T_I, T_E, V_T, GG_{EMG}, Dia_{EMG}, or Abd_{EMG}, regardless of whether it belonged to control or B + S_{pF_L} group. ***C***, Comparison between ratio changes induced by B + S_{pF_L} in pF_V:AlstR rats at rest and in the presence of Alst. Data in ***C*** are expressed as ratios of resting values, and red horizontal dashed line represents a ratio of 1. ***D***, Table containing median, IQR, and *p* values, from data represented in ***B***. $^*p < 0.05$, $^{**}p < 0.01$, $^{***}p < 0.005$.

Hyperpolarizing pF_V neurons during B + S_{pF_L} only attenuates Abd_{EMG}

We wanted to ascertain if, and how, the pF_L and pF_V interact. Thus we hyperpolarized pF_V neurons followed by B + S_{pF_L}. In anesthetized rats at rest transfected with AlstR in the ventral parafacial, i.e., pF_V:AlstR rats (Fig. 1*ii*,*iii*), B + S_{pF_L} decreased *f* and T_I; increased T_E, V_T, Dia_{EMG}, and GG_{EMG}; and induced expiratory-related Abd_{EMG} ($n = 13$; Fig. 9*Ai*,*Bi*,*D*). The same trends ($n = 13$; Fig. 9*Aii*,*Bii*,*D*) were seen in the presence of Alst (Fig. 1*vi*,*vii*). However, in the presence of Alst following B + S_{pF_L} only the ratio change [(B + S_{pF_L} + Alst)/(Ctl + Alst)] for expiratory-related Abd_{EMG} was significantly closer to 1 than the ratio change in the absence of Alst [B + S_{pF_L}/Ctl] ($n = 13$; Fig. 9*C*,*D*). Alst in the absence of AlstRs did not affect the response to B + S_{pF_L} (see next paragraph). Thus although B + S_{pF_L} had profound effects on breathing patterns, the sole effect of hyperpolarizing pF_V neurons was to reduce the B + S_{pF_L}-induced increase in expiratory-related Abd_{EMG}.

Alst does not affect the response to B + S_{pF_L} in the absence of AlstRs

In anesthetized rats at rest with no AlstRs, i.e., pF_L:HM_4DR rats (Fig. 1*i*), B + S_{pF_L} decreased *f* ($p = 0.02$) and T_I ($p = 0.04$);

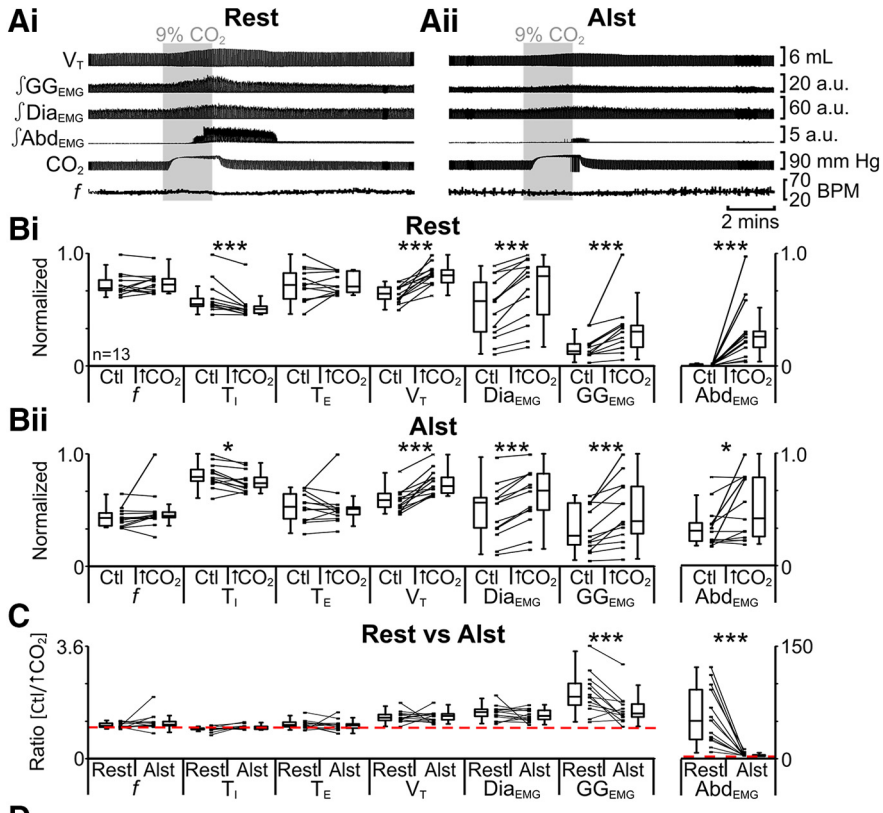

Values: median, IQR	f (breath/min)	T_I (secs)	T_E (secs)	V_T (mL)	Dia_{EMG}	GG_{EMG}	Abd_{EMG}
Rest	43.2, 5.8	0.33, 0.04	1.0, 0.3	3.9, 0.6	23.5, 18.3	12.0, 9.1	0.2, 0.1
CO_2	45.4, 7.4	0.30, 0.04	1.0, 0.3	4.9, 0.7	32.7, 17.7	29.8, 19.9	3.6, 2.0
P=	0.9	0.0009	0.8	0.0005	0.0001	0.0001	0.0001
Alst	47.1, 12.6	0.30, 0.04	1.0, 0.4	3.4, 0.7	23.2, 11.3	11.9, 16.9	0.2, 0.1
Alst CO_2	49.2, 5.5	0.28, 0.03	1.0, 0.1	4.1, 0.8	27.7, 13.5	17.9, 19.2	0.3, 0.4
P=	0.1	0.02	0.8	0.0002	0.0001	0.0006	0.04
Ratio (CO_2)	1.0, 0.1	0.9, 0.0	1.0, 0.1	1.3, 0.2	1.4, 0.2	1.9, 0.7	19.7, 26.4
Ratio (Alst CO_2)	1.0, 0.1	0.9, 0.1	1.0, 0.1	1.3, 0.2	1.3, 0.3	1.4, 0.4	1.2, 0.7
P=	0.4	0.1	0.2	0.7	0.6	0.003	0.0002

Figure 10. Hyperpolarizing pF_V neurons reduced effects of hypercapnia (9% CO_2) on Abd_{EMG} and GG_{EMG}. ***A***, Integrated traces from a single experiment: shaded area shows period of hypercapnia. ***Ai***, Rest. ***Aii***, After addition of Alst into pF_V (present for entire trace). ***B***, Comparison of respiratory variables before and after hypercapnia in pF_V:AlstR rats at rest (***Bi***) and in the presence of Alst (***Bii***). Lines connect data from individual experiments, and box-and-whisker plots show combined data. Data in ***Bi*** and ***Bii*** are normalized to highest value for that parameter, i.e., *f*, T_I, T_E, V_T, GG_{EMG}, Dia_{EMG}, or Abd_{EMG}, regardless of whether it belonged to control or 9% CO_2 group. ***C***, Comparison between ratio changes induced by hypercapnia in pF_V:AlstR rats at rest and in the presence of Alst. Data in ***C*** are expressed as ratios of resting values, and red horizontal dashed line represents a ratio of 1. ***D***, Table containing median, IQR, and *p* values, from data represented in ***B***. $*p < 0.05$, $**p < 0.01$, $***p < 0.005$.

with AlstR in the ventral parafacial, i.e., pF_V:AlstR rats (Fig. 1*ii*,*iii*), hypercapnia did not affect *f*; decreased T_I; did not affect T_E; increased V_T, Dia_{EMG}, and GG_{EMG}; and induced expiratory-related Abd_{EMG} ($n = 13$; Fig. 10*Ai*,*Bi*,*D*). The same trends ($n = 13$; Fig. 10*Aii*,*Bii*,*D*) were seen in the presence of Alst (Fig. 1*vi*,*vii*). However, in the presence of Alst during hypercapnia, only the ratio changes [(hypercapnia + Alst)/(Ctl + Alst)] for inspiratory-related GG_{EMG} and expiratory-related Abd_{EMG} were significantly closer to 1 than the ratio changes in the absence of Alst [hypercapnia/Ctl] ($n = 13$; Fig. 10*C*,*D*). Alst in the absence of AlstRs did not affect the response to hypercapnia (see next paragraph). Thus hyperpolarizing pF_V neurons during hypercapnia decreased both inspiratory-related GG_{EMG} and expiratory-related Abd_{EMG} activity.

Alst does not affect the response to hypercapnia in the absence of AlstRs

In anesthetized rats at rest with no AlstRs, i.e., pF_L:HM_4DR rats (Fig. 1*i*), hypercapnia did not affect *f* ($p = 0.8$); decreased T_I ($p = 0.04$); did not affect T_E ($p = 0.3$); increased V_T ($p = 0.02$), Dia_{EMG} ($p = 0.02$), and GG_{EMG} ($p = 0.02$); and induced expiratory-related Abd_{EMG} ($p = 0.02$; $n = 7$; data not shown). The same trends ($n = 7$; *f*: $p = 0.9$; T_I: $p = 0.02$; T_E: $p = 0.8$; V_T: $p = 0.02$; Dia_{EMG}: $p = 0.02$; GG_{EMG}: $p = 0.02$; Abd_{EMG}: $p = 0.02$; data not shown) were seen in the presence of Alst (Fig. 1*v*). Importantly, in the presence of Alst during hypercapnia, the ratio changes [(hypercapnia + Alst)/(Ctl + Alst)] for all measured variables was not significantly different to those in the absence of Alst [hypercapnia/Ctl] ($n = 7$; *f*: $p = 0.5$; T_I: $p = 0.2$; T_E: $p = 0.3$; V_T: $p = 0.08$; Dia_{EMG}: $p = 0.4$; GG_{EMG}: $p = 0.5$; Abd_{EMG}: $p = 0.7$; data not shown). Thus Alst in the absence of AlstR did not affect the response to hypercapnia.

increased T_E ($p = 0.008$), V_T ($p = 0.02$), Dia_{EMG} ($p = 0.008$), and GG_{EMG} ($p = 0.008$); and induced expiratory-related Abd_{EMG} ($p = 0.008$; $n = 7$; data not shown). The same trends ($n = 7$; *f*: $p = 0.02$; T_I: $p = 0.04$; T_E: $p = 0.008$; V_T: $p = 0.02$; Dia_{EMG}: $p = 0.008$; GG_{EMG}: $p = 0.008$; Abd_{EMG}: $p = 0.008$; data not shown) were seen in the presence of Alst (Fig. 1*v*). Importantly, in the presence of Alst following B + S_{pF_L}, the ratio changes [(B + S_{pF_L} + Alst)/(Ctl + Alst)] for all measured variables were not significantly different to the ratio changes in the absence of Alst [B + S_{pF_L}/Ctl] ($n = 7$; *f*: $p = 0.5$; T_I: $p = 0.6$; T_E: $p = 0.8$; V_T: $p = 0.8$; Dia_{EMG}: $p = 0.3$; GG_{EMG}: $p = 0.6$; Abd_{EMG}: $p = 0.8$; data not shown). Thus Alst in the absence of AlstRs did not affect the response to B + S_{pF_L}.

Hyperpolarizing pF_V neurons during hypercapnia attenuates GG_{EMG} and Abd_{EMG}

To assess the role of the pF_V in chemoreflexes, we first tested the response to hypercapnia. In anesthetized rats at rest transfected

Hyperpolarizing pF_V neurons during hypoxia attenuates GG_{EMG} and Abd_{EMG}

Using a similar sequence of protocols, we next tested the effect of hypoxia at rest. In anesthetized rats at rest transfected with AlstR in the ventral parafacial, i.e., pF_V:AlstR rats (Fig. 1*ii*,*iii*) under resting conditions, hypoxia increased *f*; decreased T_I and T_E; increased V_T, Dia_{EMG}, and GG_{EMG}; and induced expiratory-related Abd_{EMG} ($n = 13$; Fig. 11*Ai*,*Bi*,*D*). The same trends ($n = 13$; Fig. 11*Aii*,*Bii*,*D*) were seen in the presence of Alst (Fig. 1*vi*,*vii*). However, in the presence of Alst during hypoxia, only the ratio changes [(hypoxia + Alst)/(Ctl + Alst)] for inspiratory-related GG_{EMG} and expiratory-related Abd_{EMG} were significantly closer to 1 than the ratio changes in the absence of Alst [hypoxia/Ctl] ($n = 13$; Fig. 11*C*,*D*). Alst in the absence of AlstRs did not affect the response to hypoxia (see next paragraph). Thus hyperpolar-

izing pF_V neurons during hypoxia decreased both inspiratory-related GG_{EMG} and expiratory-related Abd_{EMG} activity.

Alst does not affect the response to hypoxia in the absence of AlstRs

In anesthetized rats at rest with no AlstRs, i.e., pF_L:HM_4DR rats (Fig. 1*i*), hypoxia increased *f* ($p = 0.02$); decreased T_I ($p = 0.02$) and T_E ($p = 0.02$); increased V_T ($p = 0.03$), Dia_{EMG} ($p = 0.03$), and GG_{EMG} ($p = 0.02$); and induced expiratory-related Abd_{EMG} activity ($p = 0.02$; $n = 7$; data not shown). The same trends ($n = 7$; *f*: $p = 0.02$; T_I: $p = 0.01$; T_E: $p = 0.02$; V_T: $p = 0.02$; Dia_{EMG}: $p = 0.02$; GG_{EMG}: $p = 0.008$; Abd_{EMG}: $p = 0.02$; data not shown) were seen in the presence of Alst (Fig. 1*v*). Importantly, in the presence of Alst, during hypoxia, the ratio changes [(hypoxia + Alst)/(Ctl + Alst)] for all measured variables were not significantly different to those in the absence of Alst [hypoxia/Ctl] ($n = 7$; *f*: $p = 1.0$; T_I: $p = 0.3$; T_E: $p = 1.0$; V_T: $p = 0.8$; Dia_{EMG}: $p = 0.2$; GG_{EMG}: $p = 0.2$; Abd_{EMG}: $p = 0.2$; data not shown). Thus Alst in the absence of AlstR did not affect the response to hypoxia.

AlstR and HM_4DR are equally effective in our experimental paradigms

Differences in the effects of hyperpolarizing pF_V or pF_L neurons could be due to the differences in the effects of activating HM_4DRs versus AlstRs, and not a functional distinction between pF_V and pF_L. To assess this, we transfected the pF_V with HM_4DRs.

We first tested the response to hypercapnia. In anesthetized rats at rest transfected with HM_4DR in the ventral parafacial, i.e., pF_V:HM_4DR rats (Fig. 1*iv*,*xii*), hypercapnia did not affect *f*; decreased T_I; did not affect T_E; increased V_T, Dia_{EMG}, and GG_{EMG}; and induced expiratory-related Abd_{EMG} ($n = 13$; Fig. 12*Ai*,*Bii*,*D*). The same trends ($n = 13$; Fig. 12*Aii*,*Bii*,*D*) were seen in the presence of CNO (Fig. 1*viii*). However, in the presence of CNO, during hypercapnia, only the ratio changes [(hypercapnia + CNO)/(Ctl + CNO)] for inspiratory-related GG_{EMG} and expiratory-related Abd_{EMG} were significantly closer to 1 than the ratio changes in the absence of CNO [hypercapnia/Ctl] ($n = 13$; Fig. 12*C*,*D*). Thus hyperpolarizing pF_V:HM_4DR neurons during hypercapnia affected both inspiratory-related GG_{EMG} and expiratory-related Abd_{EMG}. Regardless of whether the pF_V neurons were hyperpolarized via the activation of AlstRs or HM_4DRs, the ratio changes, i.e., [(hypercapnia + Alst)/(Ctl + Alst)] vs [(hypercapnia + CNO)/(Ctl + CNO)], were similar for inspiratory-related GG_{EMG} ($n = 21$; pF_V:AlstR: 1.4 IQR 0.4; pF_V:HM_4DR: 1.6 IQR 0.7; Kruskal–Wallis; $p = 0.7$; data not shown) and expiratory-related Abd_{EMG} ($n = 21$; pF_V:AlstR: 1.2 IQR 0.7; pF_V:HM_4DR: 1.6 IQR 1.6; Kruskal–Wallis; $p = 0.2$; data not shown).

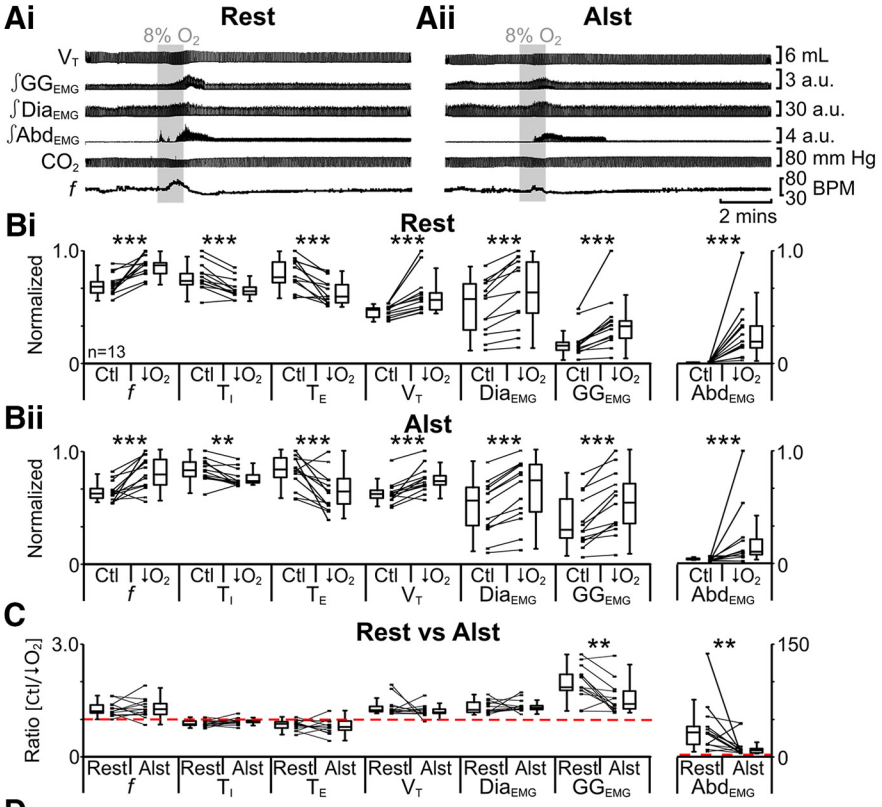

D

Values: median, IQR	*f* (breath/min)	T_I (secs)	T_E (secs)	V_T (mL)	Dia_{EMG}	GG_{EMG}	Abd_{EMG}
Rest	43.6, 6.4	0.34, 0.05	1.0, 0.2	4.1, 0.7	23.7, 17.3	13.0, 6.2	0.2, 0.1
8% O_2	56.0, 6.3	0.30, 0.03	0.8, 0.2	4.8, 1.3	26.0, 19.1	28.3, 13.6	4.7, 4.7
P=	0.0004	0.0006	0.0006	0.0002	0.0001	0.0001	0.001
Alst	42.7, 6.1	0.30, 0.05	1.1, 0.2	3.5, 0.4	23.3, 14.7	12.4, 15.3	0.2, 0.1
Alst 8% O_2	54.8, 16.0	0.27, 0.03	0.8, 0.3	4.2, 0.5	31.3, 18.3	22.9, 15.6	0.8, 1.3
P=	0.002	0.01	0.004	0.0005	0.0001	0.0001	0.002
Ratio (8% O_2)	1.2, 0.2	0.9, 0.1	0.9, 0.2	1.2, 0.2	1.2, 0.3	1.8, 0.4	28.1, 23.7
Ratio (Alst 8% O_2)	1.3, 0.3	0.9, 0.1	0.8, 0.2	1.2, 0.1	1.3, 0.1	1.4, 0.5	4.8, 5.8
P=	0.8	0.09	0.5	0.5	0.6	0.006	0.01

Figure 11. Hyperpolarizing pF_V neurons reduced effects of hypoxia (8% O_2) on Abd_{EMG} and GG_{EMG}. ***A***, Integrated traces from a single experiment: shaded area shows period of hypoxia. ***Ai***, Rest. ***Aii***, After addition of Alst into pF_V (present for entire trace). ***B***, Comparison of respiratory variables before and after hypoxia in pF_V:AlstR rats at rest (***Bi***) and in the presence of Alst (***Bii***). Lines connect data from individual experiments, and box-and-whisker plots show combined data. Data in ***Bi*** and ***Bii*** are normalized to highest value for that parameter, i.e., *f*, T_I, T_E, V_T, GG_{EMG}, Dia_{EMG}, or Abd_{EMG}, regardless of whether it belonged to control or 8% O_2 group. ***C***, Comparison between ratio changes induced by hypoxia in pF_V:AlstR rats at rest and in the presence of Alst. Data in ***C*** are expressed as ratios of resting values, and red horizontal dashed line represents a ratio of 1. ***D***, Table containing median, IQR, and *p* values, from data represented in ***B***. $^*p < 0.05$, $^{**}p < 0.01$, $^{***}p < 0.005$.

Using a similar sequence of protocols, we next tested the effect of hypoxia. In anesthetized rats at rest transfected with HM_4DR in the ventral parafacial, i.e., pF_V:HM_4DR rats (Fig. 1*iv*,*xii*), hypoxia increased *f*; decreased T_I and T_E; increased V_T, Dia_{EMG}, and GG_{EMG}; and induced expiratory-related Abd_{EMG} ($n = 13$; Fig. 13*Ai*,*Bi*,*D*). The same trends ($n = 13$; Fig. 13*Aii*,*Bii*,*D*) were seen in the presence of CNO (Fig. 1*viii*). However, in the presence of CNO, during hypoxia, only the ratio changes [(hypoxia + CNO)/(Ctl + CNO)] for inspiratory-related GG_{EMG} and expiratory-related Abd_{EMG} were significantly closer to 1 than the ratio changes in the absence of CNO [hypoxia/Ctl] ($n = 13$; Fig. 13*C*,*D*). Thus similar to hypercapnia, hyperpolarizing pF_V:HM_4DR neurons with CNO attenuated the effects of hypoxia on active expiration as well as inspiration. Regardless of whether pF_V neurons were hyperpolarized via the activation of AlstRs or HM_4DRs, the ratio changes, i.e., [(hypoxia + Alst)/(Ctl + Alst)] vs [(hypoxia + CNO)/(Ctl + CNO)], were similar for inspiratory-related GG_{EMG} ($n = 21$; pF_V:AlstR: 1.3 IQR 0.5; pF_V:

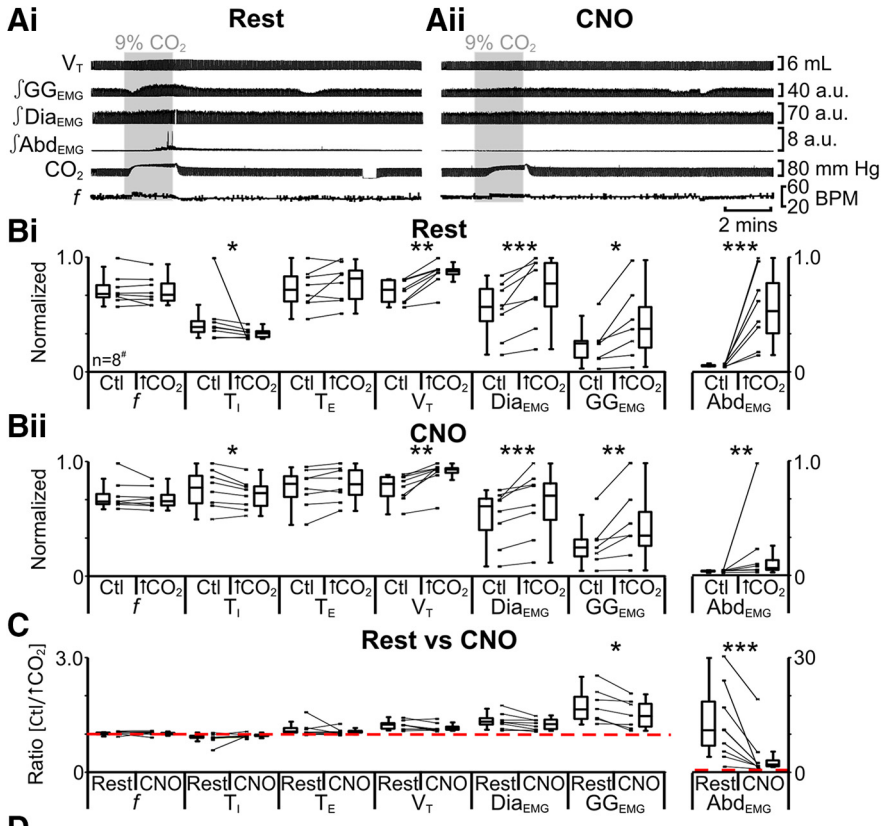

D

Values: median, IQR	*f* (breath/min)	T_I (secs)	T_E (secs)	V_T (mL)	Dia_{EMG}	GG_{EMG}	Abd_{EMG}
Rest	41.0, 6.6	0.32, 0.08	1.1, 0.3	4.3, 1.2	29.4, 15.1	12.5, 7.1	0.2, 0.0
CO_2	40.7, 9.3	0.27, 0.04	1.2, 0.4	5.3, 0.3	40.2, 20.2	18.7, 17.3	2.0, 1.7
P=	0.8	0.03	0.1	0.008	0.004	0.02	0.008
CNO	40.5. 5.5	0.29. 0.09	1.2. 0.3	4.3. 0.9	36.4. 16.0	11.4. 6.4	0.2. 0.0
CNO CO_2	40.9. 5.8	0.27. 0.06	1.2. 0.3	5.0. 0.2	41.7. 18.5	16.0. 13.1	0.3. 0.3
P=	0.2	0.03	0.07	0.008	0.004	0.008	0.01
Ratio (CO_2)	1.0, 0.0	0.9, 0.1	1.0, 0.1	1.2, 0.2	1.3, 0.2	1.6, 0.6	10.7, 11.8
Ratio (CNO CO_2)	1.0. 0.0	0.9. 0.0	1.0. 0.1	1.1. 0.1	1.2. 0.3	1.5. 0.6	1.6. 1.5
P=	0.6	0.055	0.6	0.3	0.055	0.02	0.008

Figure 12. Hyperpolarizing pF_V neurons during hypercapnia (9% CO_2) with HM_4DR only affects GG_{EMG} and Abd_{EMG}. ***A***, Integrated traces from a single experiment: shaded area shows period of hypercapnia. ***Ai***, Rest. ***Aii***, During application of CNO to medullary surface (present for entire trace). ***B***, Comparison of respiratory variables before and after hypercapnia in pF_V:HM_4DR rats at rest (***Bi***) and in the presence of CNO (***Bii***). Lines connect data from individual experiments, and box-and-whisker plots show combined data. Data in ***Bi*** and ***Bii*** are normalized to highest value for that parameter, i.e., *f*, T_I, T_E, V_T, GG_{EMG}, Dia_{EMG}, or Abd_{EMG}, regardless of whether it belonged to control or 9% CO_2 group. ***C***, Comparison between ratio changes induced by hypercapnia in pF_V:HM_4DR rats at rest and in presence of CNO. Data in ***C*** are expressed as ratios of resting values, and red horizontal dashed line represents a ratio of 1. ***D***, Table containing median, IQR, and *p* values, from data represented in ***B***. $^*p < 0.05$, $^{**}p < 0.01$, $^{***}p < 0.005$. $^{\#}n = 7$ for GG_{EMG}.

HM_4DR: 1.6 IQR 0.5; Kruskal–Wallis; $p = 0.5$; data not shown) and expiratory-related Abd_{EMG} ($n = 21$; pF_V:AlstR: 4.8 IQR 5.8; pF_V:HM_4DR: 9.2 IQR 8.2; Kruskal–Wallis; $p = 0.2$; data not shown). Thus the disparities between the pF_L and pF_V in terms of the response to hypercapnia and hypoxia are due to functional differences between the pF_V and pF_L.

Discussion

We investigated the respective contributions of two adjacent parafacial regions in controlling breathing pattern. To do this we combined two recently developed technologies for hyperpolarizing neurons, i.e., transfection of neurons with AlstRs or HM_4DRs followed by exogenous application of their ligand (Alst or CNO), to illuminate their differences in function. By making these perturbations in the same rat we could discriminate these differences. Although we focus on breathing, this approach can be used in any region of the brain to parse out differences in function among neighboring subpopulations, and where distinguishing genetic markers can be exploited, one could discriminate between overlapping populations.

Breathing in mammals is a complex behavior with critical sites in the brainstem for rhythm and pattern generation and for sensory processing. An emerging picture is that distinct regions have specific functional roles (Feldman et al., 2013), such as in CO_2-chemoreception (Guyenet et al., 2010; Hodges and Richerson, 2010; Huckstepp and Dale, 2011; Nattie, 2011), or in generation of expiratory (Onimaru and Homma, 2003; Janczewski and Feldman, 2006; Pagliardini et al., 2011) or inspiratory (Smith et al., 1991; Tan et al., 2008) rhythm. Appropriate parcellation of distinct respiratory functions to definable brainstem regions is essential for understanding neural control of breathing. Since the identification of the parafacial RTN (Smith et al., 1989; Ellenberger and Feldman, 1990; Li et al., 1999; Mulkey et al., 2004), increasing attention has been focused on understanding its role and, as more data became available (Onimaru and Homma, 2003; Janczewski and Feldman, 2006; Feldman et al., 2009; Pagliardini et al., 2011; Tupal et al., 2014), e.g., the role of other parafacial regions. In adult rats, we found that two anatomically separate parafacial regions, the pF_V and pF_L, perform very distinct roles in control of breathing, with an overlapping role in central chemoreception.

pF_V and pF_L have different active states at rest

At rest the lack of significant expiratory pumping by abdominal muscles (Iizuka and Fregosi, 2007) can be transformed into active expiration by disinhibition or photoactivation of the presumptive pF_L (Pagliardini et al., 2011). This suggests that the pF_L is silent at rest due to tonic suppression by inhibitory neurons, and that once disinhibited and/or excited, the pF_L drives active expiration (Pagliardini et al., 2011). We predicted that hyperpolarizing pF_L:HM_4DR neurons should not alter basal ventilation, and that was the case (Fig. 4).

Disinhibition in the pF_L, i.e., B + S_{pF_L}, produces expiratory-related Abd_{EMG} activity (Pagliardini et al., 2011), a reduction in *f* with a concomitant increase in V_T, and an increase in inspiratory-related Dia_{EMG} and GG_{EMG}. In pF_L:HM_4DR-transfected rats, these effects were significantly reduced following application of CNO (Fig. 5). That CNO did not completely abolish the effects of B + S_{pF_L} is likely due to incomplete transfection of pF_L neurons (~76%; Fig. 2) in the effective B + S_{pF_L} injection site and/or B + S_{pF_L} produced sufficient disinhibitory depolarization to over-

come the hyperpolarizing effects of CNO on HM_4DR-transfected neurons. We conclude that the pF_L is silent at rest due, at least in part, to postsynaptic inhibition mediated by $GABA_A$ergic and/or glycinergic receptors, but once sufficiently excited, triggers active expiration; this is consistent with our hypothesis that the pF_L is a conditional expiratory oscillator (Fig. 14; Mellen et al., 2003; Janczewski and Feldman, 2006; Pagliardini et al., 2011).

The area ventral to the facial nucleus is generally accepted to process and integrate multiple sensory inputs related to ventilation and provide a facilitatory drive to breathe (Nattie, 2000; Li et al., 2006; Moreira et al., 2007a; Mulkey et al., 2007). Consistent with previous results (Nattie and Li, 2002; Marina et al., 2010), we found that hyperpolarizing pF_V:AlstR neurons reduced basal ventilation, via a reduction in V_T due, at least in part, to attenuated Dia_{EMG} activity with no change in *f* (Fig. 8). We conclude that at rest the pF_V provides an excitatory drive to breathe (Fig. 14).

pF_V and pF_L have different roles in the response to both hypoxia and hypercapnia

In vagotomized urethane-anesthetized rats at rest, both the pF_V and pF_L are involved in responses to hypoxia and hypercapnia. The pF_V and pF_L were distinguished by their particular roles in these responses. Hyperpolarizing pF_L neurons only attenuated hypercapnia-induced (Fig. 6) and hypoxia-induced (Fig. 7) expiratory-related Abd_{EMG}, suggesting that this change is not related to the modality of the perturbation, but was specific to the initiation and maintenance of active expiration. Hyperpolarizing pF_V neurons attenuated increases in both hypercapnia-induced (Figs. 10, 12) and hypoxia-induced (Figs. 11, 13) expiratory-related Abd_{EMG} and inspiratory-related GG_{EMG}, suggesting that these changes are not related to the modality of the perturbation, but were specific to the loss of facilitatory drive affecting respiratory muscle activity. Thus when ventilatory demand increases due to changes in blood gases, the pF_L drives active expiration and the pF_V decreases airway resistance during inspiration along with a concomitant facilitatory drive that increases expiratory-related Abd_{EMG} activity (Fig. 14).

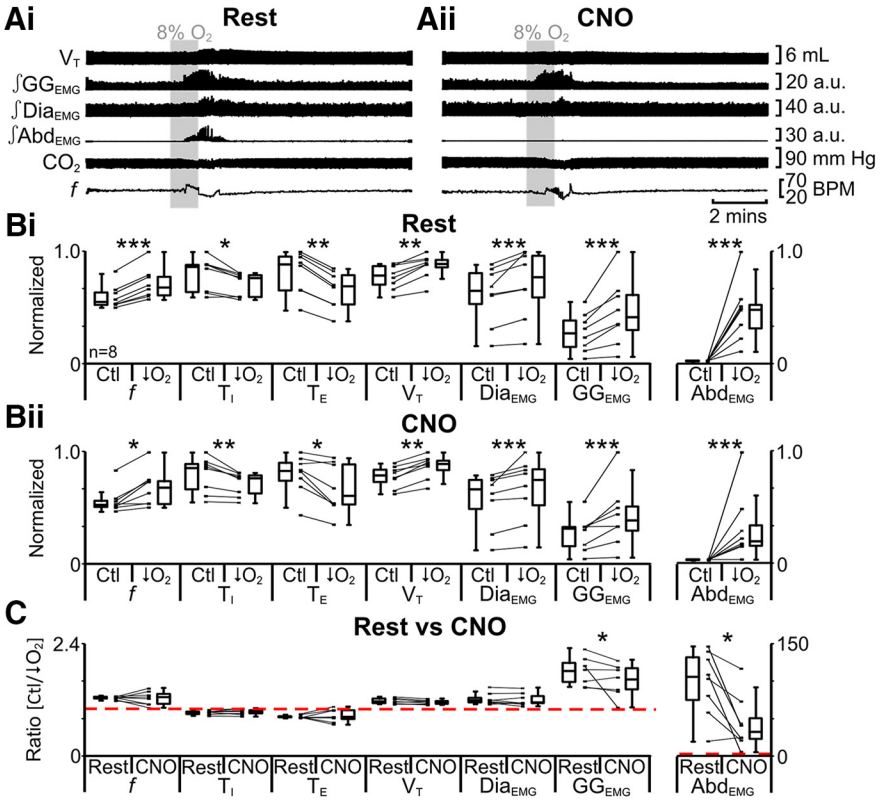

D

Values: median, IQR	*f* (breath/min)	T_I (secs)	T_E (secs)	V_T (mL)	Dia_{EMG}	GG_{EMG}	Abd_{EMG}
Rest	40.0, 8.1	0.33, 0.1	1.3, 0.4	4.4, 0.9	31.0, 13.2	13.6, 12.0	0.2, 0.1
O_2	49.3, 12.2	0.30, 0.08	1.0, 0.4	5.0, 0.4	36.8, 17.9	20.8, 16.0	5.1, 2.3
P=	0.004	0.02	0.008	0.008	0.004	0.004	0.004
CNO	39.9, 4.2	0.32, 0.09	1.2, 0.2	4.3, 0.6	34.9, 14.0	16.5, 9.3	0.2, 0.0
CNO O_2	52.0, 15.8	0.29, 0.06	0.9, 0.5	4.9, 0.5	39.4, 17.2	20.3, 11.8	1.3, 1.2
P=	0.03	0.008	0.02	0.008	0.004	0.004	0.004
Ratio (O_2)	1.2, 0.0	0.9, 0.1	0.8, 0.0	1.1, 0.1	1.2, 0.1	1.8, 0.4	31.2, 17.0
Ratio (CNO O_2)	1.2, 0.2	0.9, 0.1	0.8, 0.2	1.1, 0.1	1.1, 0.2	1.6, 0.5	9.2, 8.2
P=	1.0	0.2	0.5	0.1	0.4	0.04	0.02

Figure 13. Hyperpolarizing pF_V neurons during hypoxia (8%) with HM_4DR only affects GG_{EMG} and Abd_{EMG}. ***A***, Integrated traces from a single experiment: shaded area shows period of hypoxia. ***Ai***, Rest. ***Aii***, During application of CNO to medullary surface (present for entire trace). ***B***, Comparison of respiratory variables before and after hypoxia in pF_V:HM_4DR rats at rest (***Bi***) and in the presence of CNO (***Bii***). Lines connect data from individual experiments, and box-and-whisker plots show combined data. Data in ***Bi*** and ***Bii*** are normalized to highest value for that parameter, i.e., *f*, T_I, T_E, V_T, GG_{EMG}, Dia_{EMG}, or Abd_{EMG}, regardless of whether it belonged to control or 8% O_2 group. ***C***, Comparison between ratio changes induced by hypoxia in pF_V:HM_4DR rats at rest and in presence of CNO. Data in ***C*** are expressed as ratios of resting values, and red horizontal dashed line represents a ratio of 1. ***D***, Table containing median, IQR, and *p* values, from data represented in ***B***. $*p < 0.05$, $**p < 0.01$, $***p < 0.005$.

Further evidence the pF_L is a conditional expiratory oscillator

The pF_V contains glutamatergic neurons (Nattie and Li, 2002; Mulkey et al., 2004; Stornetta et al., 2006), lacks glycinergic neurons (Tanaka et al., 2003; Fortuna et al., 2008; Abbott et al., 2009), and is almost completely devoid of GABAergic neurons (Ellenberger, 1999; Stornetta and Guyenet, 1999; Tanaka et al., 2003). The pF_L also contains glutamatergic neurons (Onimaru et al., 2008) and lacks inhibitory neurons (Ellenberger, 1999; Stornetta and Guyenet, 1999; Tanaka et al., 2003). Thus for this discussion we consider neurons in these parafacial regions to be exclusively excitatory.

Disinhibition of the pF_L (with $B + S_{pF_L}$) reduces *f* (Fig. 5), either directly through activation of preBötC inhibitory neurons or indirectly through activation of BötC inhibitory neurons (Fig. 14). That activation of the pF_L also led to expiratory-related activity on both the Abd_{EMG} and GG_{EMG} (Fig. 5) suggests that it projects, directly or indirectly, to premotor neurons controlling the abdominal muscles (Janczewski et al., 2002) and the tongue (Fig. 14). Finally, hyperpolarizing pF_L neurons following hypoxia or hypercapnia only reduced expiratory activity, but did not affect any inspiratory parameters (Figs. 6, 7). Collectively these data are consistent with our hypothesis that the pF_L gates active expiration, most likely as a conditional expiratory oscillator (Pagliardini et al., 2011).

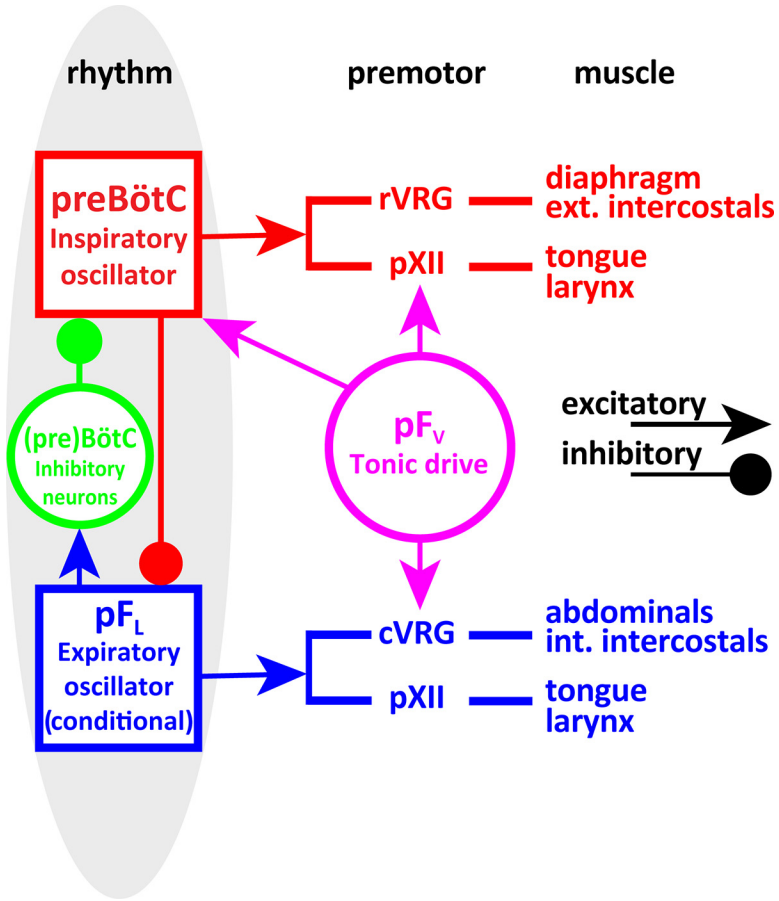

Figure 14. Schematic of minimal respiratory central pattern generator, which at its core consists of three essential components: (1) an inspiratory oscillator in preBötC that drives inspiration by exciting inspiratory premotor neuronal populations, e.g., rVRG and parahypoglossal region (pXII), and inhibits pF_L; (2) a (conditional) expiratory oscillator in pF_L that gates and drives expiration by exciting expiratory premotor neuronal populations, i.e., cVRG (Janczewski et al., 2002) and pXII, and assures alteration of phases by exciting neurons that inhibit preBötC, e.g., inhibitory neurons in either the preBötC or BötC; and (3) a source of tonic drive in pF_V that is responsive to CO_2/pH and integrates other sensory afferents affecting respiratory drive, via excitatory connections to preBötC, BötC, and respiratory premotor neurons, e.g., rVRG, cVRG, and pXII.

pF_V provides expiratory drive to breathe

Hyperpolarizing either pF_V or pF_L neurons attenuated expiratory-related Abd_{EMG}, suggesting either a direct interaction between these nuclei or a downstream convergence of their projections onto abdominal (pre)motoneurons (Janczewski et al., 2002). Due to the apparent lack of inhibitory neurons in the pF_L and pF_V (see above), if pF_V neurons project to the pF_L, hyperpolarizing pF_V neurons should attenuate all B + S_{pF_L}-induced changes in respiration; yet, hyperpolarizing pF_V neurons only reduced B + S_{pF_L}-induced expiratory-related Abd_{EMG} but not *f*, T_I, T_E, V_T, GG_{EMG}, or Dia_{EMG} (Fig. 9), supporting the idea that the pF_V modulates expiratory-related abdominal activity at the (pre)motoneuronal level, e.g., expiratory bulbospinal neurons (Janczewski et al., 2002). Importantly, the pF_V projects directly (Núñez-Abades et al., 1993; Gerrits and Holstege, 1996; Rosin et al., 2006) and indirectly, via the BötC and the parabrachial/Kölliker-fuse nuclei (Núñez-Abades et al., 1993; Rosin et al., 2006), to the caudal ventral respiratory group (cVRG; Fig. 14), which contains bulbospinal neurons projecting to spinal interneurons that in turn project to abdominal motoneurons (Iscoe, 1998; Cinelli et al., 2012), providing a pathway by which the pF_V can influence expiratory-related Abd_{EMG} activity (Fig. 14).

pF_V provides inspiratory drive

Interestingly, hyperpolarizing pF_V neurons had differential effects on the amplitude of inspiratory-related GG_{EMG} and Dia_{EMG} activities, dependent on respiratory drive, i.e., hyperpolarizing pF_V neurons at rest attenuated Dia_{EMG} (Fig. 8), whereas hyperpolarizing pF_V neurons during hypoxia or hypercapnia reduced GG_{EMG} (Figs. 9–12). This suggests that pF_V neurons that drive the diaphragm are active at rest, but that no additional pF_V neurons are recruited to drive the diaphragm during active expiration as elicited here. Conversely, neurons that drive the genioglossus are silent at rest but are recruited during active expiration. Thus different pF_V populations may separately innervate hypoglossal and phrenic premotoneurons. The pF_V (Rosin et al., 2006) and preBötC (Tan et al., 2010) both innervate a parahypoglossal region (pXII) that is most likely the premotor relay for inspiratory drive to the XII nucleus (Chamberlin et al., 2007). This provides a neural pathway by which the pF_V may alter the amplitude of GG_{EMG} independent of the actions of the preBötC (Fig. 14). Similarly, both the pF_V (Núñez-Abades et al., 1993; Rosin et al., 2006) and preBötC (Tan et al., 2010) project to the rostral VRG (rVRG), the premotor bulbospinal relay for inspiratory drive to the phrenic nucleus (Portillo and Núñez-Abades, 1992). This provides a neural pathway by which the pF_V can affect Dia_{EMG} independent of the actions of the preBötC (Fig. 14). Therefore we propose that the pF_V can influence inspiratory-related Dia_{EMG} and GG_{EMG} activity at the premotoneuronal level, i.e., pXII and rVRG, in addition to any effects mediated by projections to the preBötC (Smith et al., 1989; Ellenberger and Feldman, 1990; Rosin et al., 2006; Abbott et al., 2011; Takakura et al., 2014; Fig. 14).

Summary

pF_L neurons have characteristics consistent with their acting as an expiratory oscillator. At rest, in the absence of active expiration (Sherrey et al., 1988; Iizuka and Fregosi, 2007; Marina et al., 2010; Pagliardini et al., 2011), the activity of pF_L neurons is not expiratory modulated (Pagliardini et al., 2011); when disinhibited, or excited, active expiration is induced and many pF_L neurons become expiratory modulated (Pagliardini et al., 2011). Consistent with these observations, hyperpolarizing pF_L neurons affects expiratory-related activity, but not inspiratory-related activity. pF_V neurons are different. They are active at rest (Mulkey et al., 2004; Moreira et al., 2007b; Stornetta et al., 2009), where they provide excitatory input to the phrenic nerve (Marina et al., 2010) that affects V_T (Nattie and Li, 2002; Li et al., 2006). Consistent with this observation is that hyperpolarizing pF_V neurons reduced Dia_{EMG} amplitude; excitation of pF_V neurons sufficient to increase inspiratory activity does not induce active expiration

(Pagliardini et al., 2011, their Fig. 5). When the drive to breathe increases, i.e., during hypoxia and hypercapnia, hyperpolarizing pF_V neurons affect both inspiratory-related GG_{EMG} and expiratory-related Abd_{EMG} amplitude. Hyperpolarizing pF_V neurons did not affect *f* under any state tested, similar to previous reports involving silencing, or destruction, of presumptive pF_V neurons (Nattie and Li, 2002; Marina et al., 2010). Thus, the pF_V appears to provide a generic facilitatory drive to respiratory-related (pre)motoneurons that does not affect frequency.

In conclusion, by differentially decreasing the excitability of neighboring parafacial regions, we identify two distinct functional parafacial regions: the pF_L is a conditional expiratory oscillator, and the pF_V provides a generic facilitatory drive to respiration. We postulate that central pattern generation for breathing has (at least) three essential functional components associated with specific sites in the brainstem: (1) an inspiratory oscillator in the preBötC, (2) a (conditional) expiratory oscillator in the pF_L, and (3) a source of respiratory drive related to chemosensory and likely descending inputs (such as related to exercise) in the pF_V (Fig. 14).

Notes

Supplemental material for this article is available at http://feldmanlab.neurobio.ucla.edu. Supplemental information contains figures and legends for control experiments involving CNO and Alst. This material has not been peer reviewed.

References

Abbott SB, Stornetta RL, Socolovsky CS, West GH, Guyenet PG (2009) Photostimulation of channelrhodopsin-2 expressing ventrolateral medullary neurons increases sympathetic nerve activity and blood pressure in rats. J Physiol 587:5613–5631. CrossRef Medline

Abbott SB, Stornetta RL, Coates MB, Guyenet PG (2011) Phox2b-expressing neurons of the parafacial region regulate breathing rate, inspiration, and expiration in conscious rats. J Neurosci 31:16410–16422. CrossRef Medline

Birgül N, Weise C, Kreienkamp HJ, Richter D (1999) Reverse physiology in *drosophila*: identification of a novel allatostatin-like neuropeptide and its cognate receptor structurally related to the mammalian somatostatin/galanin/opioid receptor family. EMBO J 18:5892–5900. CrossRef Medline

Callaway EM (2005) A molecular and genetic arsenal for systems neuroscience. Trends Neurosci 28:196–201. CrossRef Medline

Chamberlin NL, Eikermann M, Fassbender P, White DP, Malhotra A (2007) Genioglossus premotoneurons and the negative pressure reflex in rats. J Physiol 579:515–526. CrossRef Medline

Cinelli E, Bongianni F, Pantaleo T, Mutolo D (2012) Modulation of the cough reflex by $GABA_A$ receptors in the caudal ventral respiratory group of the rabbit. Front Physiol 3:403. CrossRef Medline

Ellenberger HH (1999) Distribution of bulbospinal γ-aminobutyric acid-synthesizing neurons of the ventral respiratory group of the rat. J Comp Neurol 411:130–144. CrossRef Medline

Ellenberger HH, Feldman JL (1990) Brainstem connections of the rostral ventral respiratory group of the rat. Brain Res 513:35–42. CrossRef Medline

Feldman JL, Kam K, Janczewski WA (2009) Practice makes perfect, even for breathing. Nat Neurosci 12:961–963. CrossRef Medline

Feldman JL, Del Negro CA, Gray PA (2013) Understanding the rhythm of breathing: so near, yet so far. Annu Rev Physiol 75:423–452. CrossRef Medline

Fortuna MG, West GH, Stornetta RL, Guyenet PG (2008) Bötzinger expiratory-augmenting neurons and the parafacial respiratory group. J Neurosci 28:2506–2515. CrossRef Medline

Gerrits PO, Holstege G (1996) Pontine and medullary projections to the nucleus retroambiguus: a wheat germ agglutinin-horseradish peroxidase and autoradiographic tracing study in the cat. J Comp Neurol 373:173–185. CrossRef Medline

Guyenet PG, Stornetta RL, Bayliss DA, Mulkey DK (2005) Retrotrapezoid nucleus: a litmus test for the identification of central chemoreceptors. Exp Physiol 90:247–257. CrossRef Medline

Guyenet PG, Stornetta RL, Bayliss DA (2010) Central respiratory chemoreception. J Comp Neurol 518:3883–3906. CrossRef Medline

Hodges MR, Richerson GB (2010) Medullary serotonin neurons and their roles in central respiratory chemoreception. Respir Physiol Neurobiol 173:256–263. CrossRef Medline

Huckstepp RT, Dale N (2011) Redefining the components of central CO_2 chemosensitivity–towards a better understanding of mechanism. J Physiol 589:5561–5579. Medline

Iizuka M, Fregosi RF (2007) Influence of hypercapnic acidosis and hypoxia on abdominal expiratory nerve activity in the rat. Respir Physiol Neurobiol 157:196–205. CrossRef Medline

Iscoe S (1998) Control of abdominal muscles. Prog Neurobiol 56:433–506. CrossRef Medline

Janczewski WA, Feldman JL (2006) Distinct rhythm generators for inspiration and expiration in the juvenile rat. J Physiol 570:407–420. Medline

Janczewski WA, Onimaru H, Homma I, Feldman JL (2002) Opioid-resistant respiratory pathway from the preinspiratory neurones to abdominal muscles: *in vivo* and *in vitro* study in the newborn rat. J Physiol 545:1017–1026. CrossRef Medline

Li A, Randall M, Nattie EE (1999) CO_2 microdialysis in retrotrapezoid nucleus of the rat increases breathing in wakefulness but not in sleep. J Appl Physiol 87:910–919. Medline

Li A, Zhou S, Nattie E (2006) Simultaneous inhibition of caudal medullary raphe and retrotrapezoid nucleus decreases breathing and the CO_2 response in conscious rats. J Physiol 577:307–318. CrossRef Medline

Luo L, Callaway EM, Svoboda K (2008) Genetic dissection of neural circuits. Neuron 57:634–660. CrossRef Medline

Marina N, Abdala AP, Trapp S, Li A, Nattie EE, Hewinson J, Smith JC, Paton JF, Gourine AV (2010) Essential role of Phox2b-expressing ventrolateral brainstem neurons in the chemosensory control of inspiration and expiration. J Neurosci 30:12466–12473. CrossRef Medline

Mellen NM, Janczewski WA, Bocchiaro CM, Feldman JL (2003) Opioid-induced quantal slowing reveals dual networks for respiratory rhythm generation. Neuron 37:821–826. CrossRef Medline

Moreira TS, Takakura AC, Colombari E, Guyenet PG (2007a) Activation of 5-hydroxytryptamine type 3 receptor-expressing C-fiber vagal afferents inhibits retrotrapezoid nucleus chemoreceptors in rats. J Neurophysiol 98:3627–3637. CrossRef Medline

Moreira TS, Takakura AC, Colombari E, West GH, Guyenet PG (2007b) Inhibitory input from slowly adapting lung stretch receptors to retrotrapezoid nucleus chemoreceptors. J Physiol 580:285–300. CrossRef Medline

Mulkey DK, Stornetta RL, Weston MC, Simmons JR, Parker A, Bayliss DA, Guyenet PG (2004) Respiratory control by ventral surface chemoreceptor neurons in rats. Nat Neurosci 7:1360–1369. CrossRef Medline

Mulkey DK, Rosin DL, West G, Takakura AC, Moreira TS, Bayliss DA, Guyenet PG (2007) Serotonergic neurons activate chemosensitive retrotrapezoid nucleus neurons by a pH-independent mechanism. J Neurosci 27:14128–14138. CrossRef Medline

Nattie E (2000) Multiple sites for central chemoreception: their role in response sensitivity and in sleep and wakefulness. Respir Physiol 122:223–235. CrossRef Medline

Nattie E (2011) Julius H. Comroe, Jr., Distinguished lecture: central chemoreception: then …and now. J Appl Physiol 110:1–8. CrossRef Medline

Nattie EE, Li A (2002) Substance P-saporin lesions of neurons with NK1 receptors in one chemosensitive site in rats decreases ventilation and chemosensitivity. J Physiol 544:603–616. CrossRef Medline

Nawaratne V, Leach K, Suratman N, Loiacono RE, Felder CC, Armbruster BN, Roth BL, Sexton PM, Christopoulos A (2008) New insights into the function of M4 muscarinic acetylcholine receptors gained using a novel allosteric modulator and a DREADD (Designer Receptor Exclusively Activated by a Designer Drug). Mol Pharmacol 74:1119–1131. CrossRef Medline

Núñez-Abades PA, Morillo AM, Pásaro R (1993) Brainstem connections of the rat ventral respiratory subgroups: afferent projections. J Auton Nerv Syst 42:99–118. CrossRef Medline

Oku Y, Masumiya H, Okada Y (2007) Postnatal developmental changes in activation profiles of the respiratory neuronal network in the rat ventral medulla. J Physiol 585:175–186. CrossRef Medline

Onimaru H, Homma I (2003) A novel functional neuron group for respira-

tory rhythm generation in the ventral medulla. J Neurosci 23:1478–1486. Medline

Onimaru H, Ikeda K, Kawakami K (2008) CO_2-sensitive preinspiratory neurons of the parafacial respiratory group express Phox2b in the neonatal rat. J Neurosci 28:12845–12850. CrossRef Medline

Pagliardini S, Janczewski WA, Tan W, Dickson CT, Deisseroth K, Feldman JL (2011) Active expiration induced by excitation of ventral medulla in adult anesthetized rats. J Neurosci 31:2895–2905. CrossRef Medline

Pei Y, Rogan SC, Yan F, Roth BL (2008) Engineered GPCRs as tools to modulate signal transduction. Physiology 23:313–321. CrossRef Medline

Portillo F, Núñez-Abades A (1992) Distribution of bulbospinal neurones supplying bilateral innervation to the phrenic nucleus in the rat. Brain Res 583:349–355. CrossRef Medline

Putnam RW, Conrad SC, Gdovin MJ, Erlichman JS, Leiter JC (2005) Neonatal maturation of the hypercapnic ventilatory response and central neural CO_2 chemosensitivity. Respir Physiol Neurobiol 149:165–179. CrossRef Medline

Ray RS, Corcoran AE, Brust RD, Kim JC, Richerson GB, Nattie E, Dymecki SM (2011) Impaired respiratory and body temperature control upon acute serotonergic neuron inhibition. Science 333:637–642. CrossRef Medline

Rosin DL, Chang DA, Guyenet PG (2006) Afferent and efferent connections of the rat retrotrapezoid nucleus. J Comp Neurol 499:64–89. CrossRef Medline

Sherrey JH, Pollard MJ, Megirian D (1988) Proprioceptive, chemoreceptive and sleep state modulation of expiratory muscle activity in the rat. Exp Neurol 101:50–62. CrossRef Medline

Smith JC, Morrison DE, Ellenberger HH, Otto MR, Feldman JL (1989) Brainstem projections to the major respiratory neuron populations in the medulla of the cat. J Comp Neurol 281:69–96. CrossRef Medline

Smith JC, Ellenberger HH, Ballanyi K, Richter DW, Feldman JL (1991) Pre-Bötzinger Complex: a brainstem region that may generate respiratory rhythm in mammals. Science 254:726–729. CrossRef Medline

Stornetta RL, Guyenet PG (1999) Distribution of glutamic acid decarboxylase mRNA-containing neurons in rat medulla projecting to thoracic spinal cord in relation to monoaminergic brainstem neurons. J Comp Neurol 407:367–380. CrossRef Medline

Stornetta RL, Moreira TS, Takakura AC, Kang BJ, Chang DA, West GH, Brunet JF, Mulkey DK, Bayliss DA, Guyenet PG (2006) Expression of Phox2b by brainstem neurons involved in chemosensory integration in the adult rat. J Neurosci 26:10305–10314. CrossRef Medline

Stornetta RL, Spirovski D, Moreira TS, Takakura AC, West GH, Gwilt JM, Pilowsky PM, Guyenet PG (2009) Galanin is a selective marker of the retrotrapezoid nucleus in rats. J Comp Neurol 512:373–383. CrossRef Medline

Stunden CE, Filosa JA, Garcia AJ, Dean JB, Putnam RW (2001) Development of *in vivo* ventilatory and single chemosensitive neuron response to hypercapnia in rats. Respir Physiol 127:135–155. CrossRef Medline

Takakura AC, Barna BF, Cruz JC, Colombari E, Moreira TS (2014) Phox2b-expressing retrotrapezoid neurons and the integration of central and peripheral chemosensory control of breathing in conscious rats. Exp Physiol 99:571–585. CrossRef Medline

Tan EM, Yamaguchi Y, Horwitz GD, Gosgnach S, Lein ES, Goulding M, Albright TD, Callaway EM (2006) Selective and quickly reversible inactivation of mammalian neurons in vivo using the *Drosophila* allatostatin receptor. Neuron 51:157–170. CrossRef Medline

Tan W, Janczewski WA, Yang P, Shao XM, Callaway EM, Feldman JL (2008) Silencing preBötzinger complex somatostatin-expressing neurons induces persistent apnea in awake rat. Nat Neurosci 11:538–540. CrossRef Medline

Tan W, Pagliardini S, Yang P, Janczewski WA, Feldman JL (2010) Projections of preBötzinger Complex neurons in adult rats. J Comp Neurol 518:1862–1878. CrossRef Medline

Tanaka I, Ezure K, Kondo M (2003) Distribution of glycine transporter 2 mRNA-containing neurons in relation to glutamic acid decarboxylase mRNA-containing neurons in rat medulla. Neurosci Res 47:139–151. CrossRef Medline

Tupal S, Huang WH, Picardo MC, Ling GY, Del Negro CA, Zoghbi HY, Gray PA, Calabrese RL (2014) Atoh1-dependent rhombic lip neurons are required for temporal delay between independent respiratory oscillators in embryonic mice. eLife 3:e02265. CrossRef Medline

Yuste R (2008) Circuit neuroscience: the road ahead. Front Neurosci 2:6–9. CrossRef Medline